

Closed Sub-Monodromy Problems, Local Mirror Symmetry and Branes on Orbifolds

Kenji Mohri, Yoko Onjo and Sung-Kil Yang

*Institute of Physics, University of Tsukuba
Ibaraki 305-8571, Japan*

Abstract

We study D-branes wrapping an exceptional four-cycle $\mathbf{P}(1, a, b)$ in a blown-up $\mathbf{C}^3/\mathbf{Z}_m$ non-compact Calabi–Yau threefold with $(m; a, b) = (3; 1, 1), (4; 1, 2)$ and $(6; 2, 3)$. In applying the method of local mirror symmetry we find that the Picard–Fuchs equations for the local mirror periods in the $\mathbf{Z}_{3,4,6}$ orbifolds take the same form as the ones in the local $E_{6,7,8}$ del Pezzo models, respectively. It is observed, however, that the orbifold models and the del Pezzo models possess different physical properties because the background NS B-field is turned on in the case of $\mathbf{Z}_{3,4,6}$ orbifolds. This is shown by analyzing the periods and their monodromies in full detail with the help of Meijer G-functions. We use the results to discuss D-brane configurations on $\mathbf{P}(1, a, b)$ as well as on del Pezzo surfaces. We also discuss the number theoretic aspect of local mirror symmetry and observe that the exponent which governs the exponential growth of the Gromov–Witten invariants is determined by the special value of the Dirichlet L -function.

Contents

1	Introduction	1
2	Picard–Fuchs equations for local Calabi–Yau	3
2.1	Toric geometry of orbifolds	3
2.2	GKZ equations for orbifolds	5
2.3	Three distinguished models	7
2.4	Picard–Fuchs equations for local del Pezzo models	8
3	Solutions of Picard–Fuchs equations	10
3.1	Solutions at $z = 0$	12
3.2	Solutions at $z = \infty$	13
3.3	Solutions at $z = 1$	14
3.3.1	Solutions from the recursion relation	14
3.3.2	Torus periods	15
3.3.3	Solutions based on torus periods	17
4	Mirror maps and modular functions	21
4.1	Mirror maps for local Calabi–Yau	22
4.2	Mirror map for tori	23
4.3	Gromov–Witten invariants	25
4.4	Local mirror from Mahler measure	27
4.5	Monodromy matrices	31
5	D-branes wrapping a surface	33
5.1	Local del Pezzo models	34
5.2	Orbifold models	37
5.3	Monodromy invariant intersection form	41
	Appendix A Exceptional bundles on \mathbf{P}^2	42

1 Introduction

Type II string compactification has aroused a great deal of interest in D-branes on Calabi–Yau space [1]. Among recent works [2]–[13], Diaconescu and Gomis studied the blown-up $\mathbf{C}^3/\mathbf{Z}_3$ model [3] and found an interesting correspondence between \mathbf{Z}_3 fractional branes at the orbifold point and wrapped BPS D-branes on an exceptional \mathbf{P}^2 cycle. The spectrum of BPS D-branes is studied further in [9, 10]. As demonstrated in these papers, blown-up

orbifolds as models of Calabi–Yau threefolds are worth of being considered since they admit an exact description in terms of CFT at the orbifold point in the Kähler moduli space which parameterizes the size of exceptional four-cycles, while the large radius behavior of D-branes wrapped on exceptional cycles can be analyzed by invoking local mirror symmetry [14]. Our purpose in this paper is to generalize [3] and consider a blown-up $\mathbf{C}^3/\mathbf{Z}_m$ model with $m = 3, 4, 6$ in which there exists an exceptional divisor \mathbf{P}^2 , $\mathbf{P}(1, 1, 2)$ and $\mathbf{P}(1, 2, 3)$, respectively.

The paper is organized and summarized as follows:

In section 2, we start with reviewing a toric description of the blown-ups of orbifolds $\mathbf{C}^3/\mathbf{Z}_m$, and introduce GKZ equations for the purpose of applying local mirror symmetry. It is seen that our $\mathbf{Z}_{3,4,6}$ orbifold models are three particular examples of non-compact Calabi–Yau threefolds $\mathcal{O}_{\mathbf{P}(1,a,b)}(-m)$ with $m = 1 + a + b$. Upon formulating sub-monodromy problems based on the GKZ equations, we observe that the $\mathbf{Z}_{3,4,6}$ orbifold models and the local $E_{6,7,8}$ del Pezzo models share the Picard–Fuchs equations which are closely related to the $E_{6,7,8}$ elliptic singularities.

In section 3, the detailed analysis of the solutions to the Picard–Fuchs equations is presented. Especially we employ Meijer G-functions in constructing solutions as they provide the natural basis to determine the mirror map. Moreover, remarkable relations between the special values of G-functions and zeta functions are observed. This point is considered further in the next section.

In section 4, the mirror maps for the orbifold models and the local del Pezzo models are obtained. It is seen clearly that the difference between the two models lies in the dependence on the background NS B-field; the B-field is non-vanishing for the orbifold models, whereas $B = 0$ for the del Pezzo models. We then describe the computation of Gromov–Witten invariants of the models, putting emphasis on the relation to modular functions. We also discuss our observation which reveals some arithmetic properties of local mirror symmetry in view of the relation between the special values of zeta functions and the Mahler measure in number theory.

In section 5, we express the BPS central charge in terms of the period integrals. It is shown that in the large radius limit the same form of the central charge (up to world-sheet instanton corrections) is derived by the geometrical consideration of relevant four-cycles

embedded in Calabi–Yau space. Combining this observation with the results obtained in the previous sections, we discuss D-brane configurations on $E_{6,7,8}$ del Pezzo surfaces and $\mathbf{P}(1, a, b)$.

In Appendix A, we review exceptional bundles on \mathbf{P}^2 which are relevant to the \mathbf{Z}_3 orbifold model.

2 Picard–Fuchs equations for local Calabi–Yau

2.1 Toric geometry of orbifolds

Let us consider the non-compact Calabi–Yau orbifold model $\mathbf{C}^3/\mathbf{Z}_m$, where the action of the cyclic group \mathbf{Z}_m on the coordinates of \mathbf{C}^3 is defined by

$$(x_1, x_2, x_3) \rightarrow (\omega x_1, \omega^a x_2, \omega^b x_3). \quad (2.1)$$

Here $\omega = e^{2\pi i/m}$ is a primitive m th root of unity and the two positive integers (a, b) must satisfy the Calabi–Yau condition $1 + a + b = m$.

Toric geometry [15, 16] is a powerful tool to describe the blow-ups of the orbifold $\mathbf{C}^3/\mathbf{Z}_m$. Let N be the rank three lattice the generators of which we denote by $\{\mathbf{e}_1, \mathbf{e}_2, \mathbf{e}_3\}$ and $M = N^*$ the dual lattice. Then $\mathbf{C}^3/\mathbf{Z}_m$ itself admits a toric description by the fan \mathcal{F} defined by a unique maximal cone in $N_{\mathbf{R}}$: $\sigma = \text{pos}\{\boldsymbol{\nu}_1, \boldsymbol{\nu}_2, \boldsymbol{\nu}_3\}$, where $\boldsymbol{\nu}_1 = -a\mathbf{e}_1 - b\mathbf{e}_2 + \mathbf{e}_3$, $\boldsymbol{\nu}_2 = \mathbf{e}_1 + \mathbf{e}_3$, $\boldsymbol{\nu}_3 = \mathbf{e}_2 + \mathbf{e}_3$, and $\text{pos}\{\mathbf{v}_i \mid i \in I\} := \bigoplus_{i \in I} \mathbf{R}_{\geq 0} \mathbf{v}_i$ means the convex polyhedral cone defined by the positive hull of the vectors inside the braces. The dual cone σ^* is the cone in $M_{\mathbf{R}}$ defined by $\{\mathbf{w} \in M_{\mathbf{R}} \mid \langle \mathbf{w}, \boldsymbol{\nu}_{1,2,3} \rangle \geq 0\}$. It can be seen that the ring of the \mathbf{Z}_m -invariant monomials, that is the affine coordinate ring of the orbifold $\mathbf{C}^3/\mathbf{Z}_m$, is isomorphic to the (additive) semi-group of the lattice points of the dual cone $M \cap \sigma^*$ by

$$M \cap \sigma^* \ni \mathbf{w} \rightarrow x_1^{\langle \mathbf{w}, \boldsymbol{\nu}_1 \rangle} x_2^{\langle \mathbf{w}, \boldsymbol{\nu}_2 \rangle} x_3^{\langle \mathbf{w}, \boldsymbol{\nu}_3 \rangle}. \quad (2.2)$$

Crepanant blow-ups of a variety are those which preserve its canonical line bundle; in particular, a crepanant blow-up of a Calabi–Yau variety respects the Calabi–Yau condition, as it is equivalent to the triviality of the canonical line bundle. For the case of our orbifold

$\mathbf{C}^3/\mathbf{Z}_m$, it is known that there is a one-to-one correspondence between the crepant divisors and the set of the lattice points

$$\{\boldsymbol{\nu} \in \sigma \cap N \mid \langle \mathbf{e}_3^*, \boldsymbol{\nu} \rangle = 1\}, \quad (2.3)$$

which are incorporated in the refinement of the fan \mathcal{F} under the corresponding blow-up.

Let us consider the crepant (partial) blow-up $\text{Bl}_{\boldsymbol{\nu}_0}(\mathbf{C}^3/\mathbf{Z}_m) \rightarrow \mathbf{C}^3/\mathbf{Z}_m$ defined by the subdivision of the cone σ by the vector $\boldsymbol{\nu}_0 := \mathbf{e}_3$ which is an element of (2.3). In the process of the blow-up, the origin $(0, 0, 0)$ is blown-up to the exceptional divisor $\mathbf{P}(1, a, b)$, and the resulting Calabi–Yau variety $\text{Bl}_{\boldsymbol{\nu}_0}(\mathbf{C}^3/\mathbf{Z}_m)$ is identified with the canonical line bundle (in the orbifold sense) of it, that is, we have

$$\text{Bl}_{\boldsymbol{\nu}_0}(\mathbf{C}^3/\mathbf{Z}_m) \cong K_{\mathbf{P}(1,a,b)} = \mathcal{O}_{\mathbf{P}(1,a,b)}(-m). \quad (2.4)$$

The fan of the blown-up orbifold $\text{Bl}_{\boldsymbol{\nu}_0}(\mathbf{C}^3/\mathbf{Z}_m)$, which we denote by $\tilde{\mathcal{F}}$, is defined by the collection of the following three maximal cones:

$$\sigma_1 = \text{pos}\{\boldsymbol{\nu}_0, \boldsymbol{\nu}_2, \boldsymbol{\nu}_3\}, \quad \sigma_2 = \text{pos}\{\boldsymbol{\nu}_0, \boldsymbol{\nu}_1, \boldsymbol{\nu}_3\}, \quad \sigma_3 = \text{pos}\{\boldsymbol{\nu}_0, \boldsymbol{\nu}_1, \boldsymbol{\nu}_2\}.$$

These maximal cones define the affine open covering $\text{Bl}_{\boldsymbol{\nu}_0}(\mathbf{C}^3/\mathbf{Z}_m) = \bigcup_{i=1}^3 U_{\sigma_i}$, where $U_{\sigma_1} \cong \mathbf{C}^3$ is a smooth patch, however the remaining two $U_{\sigma_2} \cong \mathbf{C}^3/\mathbf{Z}_a$, $U_{\sigma_3} \cong \mathbf{C}^3/\mathbf{Z}_b$ have orbifold singularities in general. The exceptional divisor $S := \mathbf{P}(1, a, b)$ is the one associated with the 1-cone $\mathbf{R}_{\geq 0}\boldsymbol{\nu}_0$ in $\tilde{\mathcal{F}}$, the toric description of which is given as follows: Let $\pi : N \rightarrow \bar{N} = N/\mathbf{Z}\mathbf{e}_3$ the quotient lattice and the canonical projection. Then the two dimensional complete fan $\bar{\mathcal{F}}$ defined by the collection of the maximal cones $\pi(\sigma_1)$, $\pi(\sigma_2)$ and $\pi(\sigma_3)$ in $\bar{N}_{\mathbf{R}}$ produces $\mathbf{P}(1, a, b)$ as the associated toric twofold. It is seen that $\mathbf{P}(1, a, b)$ has \mathbf{Z}_a and \mathbf{Z}_b orbifold singular points. We can compute its triple intersection in the blown-up orbifold:

$$S \cdot S \cdot S = c_1(S) \cdot c_1(S) = \frac{m^2}{ab}. \quad (2.5)$$

The convex polyhedron in $\bar{N}_{\mathbf{R}}$ defined by the convex hull of the three points: $\pi(\boldsymbol{\nu}_1)$, $\pi(\boldsymbol{\nu}_2)$, $\pi(\boldsymbol{\nu}_3)$, becomes a *reflexive polyhedron* only in the three cases: $\{a, b\} = \{1, 1\}$, $\{1, 2\}$, $\{2, 3\}$, when the exceptional divisor $\mathbf{P}(1, a, b)$ has as its anti-canonical divisor

an elliptic curves of the type $E_{6,7,8}$ respectively. The connection between non-compact orbifolds and elliptic curves in these distinguished models will become important when we solve the Picard–Fuchs equations of them below.

The introduction of the homogeneous coordinates (x_0, x_1, x_2, x_3) greatly simplifies the construction of the blown-up orbifold $\text{Bl}_{\nu_0}(\mathbf{C}^3/\mathbf{Z}_m)$, where each coordinate x_i corresponds to the primitive generator ν_i and the linear relation between them

$$-m\nu_0 + \nu_1 + a\nu_2 + b\nu_3 = \mathbf{0} \quad (2.6)$$

tells us the $U(1)$ charge assignment for the homogeneous coordinates:

$$(x_0; x_1, x_2, x_3) \sim (\lambda^{-m} x_0; \lambda x_1, \lambda^a x_2, \lambda^b x_3), \quad \lambda \in \mathbf{C}^*, \quad (2.7)$$

where x_0 represents the fiber direction of the orbifold line bundle (2.4), and (x_1, x_2, x_3) the homogeneous coordinates of the base twofold $\mathbf{P}(1, a, b)$. The charge vector

$$l = (l_i) = (-m; 1, a, b), \quad (2.8)$$

is called the Mori vector, from which we can write down the Picard–Fuchs equation for the local mirror periods of the blown-up orbifold $\text{Bl}_{\nu_0}(\mathbf{C}^3/\mathbf{Z}_m)$.

2.2 GKZ equations for orbifolds

There is a standard procedure to derive the Picard–Fuchs equation for the blown-up orbifold $\text{Bl}_{\nu_0}(\mathbf{C}^3/\mathbf{Z}_m)$ from its toric data [17, 18, 19, 20], which we review briefly here. First let us define the bare Kähler modulus parameter z , which controls the size of the exceptional divisor, by

$$z = \prod_{i=0}^3 \left(\frac{a_i}{l_i} \right)^{l_i} := e^\beta z_0, \quad e^\beta = \prod_{i=0}^3 |l_i^{-l_i}|, \quad (2.9)$$

where $\{a_i\}$ are the coefficients of the monomials appearing in the defining polynomial of the mirror variety, and we use either z (normalized) or z_0 (unnormalized) according to the situation. Note that the large radius region corresponds to $|z| \ll 1$, while the region with $|z| \gg 1$ is called the Landau–Ginzburg or orbifold phase. Second, given a general Mori vector (l_i) , the GKZ operator associated with it is

$$\square_l := \prod_{l_i > 0} \left(\frac{\partial}{\partial a_i} \right)^{l_i} - \prod_{l_i < 0} \left(\frac{\partial}{\partial a_i} \right)^{-l_i}. \quad (2.10)$$

In particular, for our blown-up orbifold, the use of (2.8) combined with the ansatz for a mirror period $\Pi(a_i) = f(z)$ leads to the following GKZ equation [20]:

$$\square_{\text{orb}} f(z) = 0, \quad \square_{\text{orb}} = \left\{ \prod_{k_2=0}^{a-1} \left(\Theta_z - \frac{k_2}{a} \right) \prod_{k_3=0}^{b-1} \left(\Theta_z - \frac{k_3}{b} \right) - z \prod_{k_0=1}^{m-1} \left(\Theta_z + \frac{k_0}{m} \right) \right\} \circ \Theta_z, \quad (2.11)$$

where $\Theta_z = zd/dz$ is the logarithmic differential operator as usual. Let us consider the behavior of the solutions of (2.11) around the large radius limit point $z = 0$, where we can rely on the classical geometry of the exceptional divisor $\mathbf{P}(1, a, b)$. Substituting the ansatz $f(z) = \sum_{n=0}^{\infty} f_n z^{n+\rho}$ for a solution of (2.11), we obtain the indicial equation for ρ :

$$\prod_{k_2=1}^{a-1} \left(\rho - \frac{k_2}{a} \right) \prod_{k_3=1}^{b-1} \left(\rho - \frac{k_3}{b} \right) \cdot \rho^3 = 0. \quad (2.12)$$

The triple zero at $\rho = 0$ yields the three solutions of the GKZ equation (2.11): the constant solution 1, the single- and double-log solutions, which clearly correspond to the zero-, two- and four-cycles on the exceptional divisor.

The most efficient way to obtain these solutions would be the Frobenius method [18]; We first make the formal power series

$$\hat{U}_0(z, \rho) = \sum_{n=0}^{\infty} \bar{A}(n + \rho) (e^{\epsilon\pi i} z_0)^{n+\rho}, \quad \epsilon = \begin{cases} 0, & m = \text{even}, \\ 1, & m = \text{odd}, \end{cases} \quad (2.13)$$

$$\bar{A}(n) = \frac{1}{\Gamma(-mn + 1)\Gamma(n + 1)\Gamma(an + 1)\Gamma(bn + 1)}. \quad (2.14)$$

The three solutions [†] then are recovered by the expansion in the formal variable ρ :

$$\lim_{\rho \rightarrow 0} \hat{U}_0(z, \rho) = 1, \quad \lim_{\rho \rightarrow 0} \frac{\partial}{\partial \rho} \hat{U}_0(z, \rho), \quad \lim_{\rho \rightarrow 0} \frac{1}{2} \frac{\partial^2}{\partial \rho^2} \hat{U}_0(z, \rho).$$

For completeness, we give the explicit forms of the two non-trivial solutions:

$$\hat{U}_1(z) = \log(z_0) + \sum_{n=1}^{\infty} A_0(n) z_0^n, \quad (2.15)$$

$$\hat{U}_2(z) = \frac{1}{2} \log^2(z_0) + \sum_{n=1}^{\infty} A_0(n) z_0^n \log(z_0) + \sum_{n=1}^{\infty} A_0(n) B(n) z_0^n, \quad (2.16)$$

[†]If $\{k_2/a, k_3/b\} \cap \{k_0/m\}$ is not empty, we can delete the corresponding factors from the left of the GKZ operator (2.11), to get a operator of lower rank, as we shall do in (2.20) and (2.21). The three functions 1, $\hat{U}_1(z)$, $\hat{U}_2(z)$ obtained by the Frobenius method are the solutions of this reduced GKZ equation.

where

$$A_0(n) = \frac{\Gamma(mn + 1)}{n\Gamma(n + 1)\Gamma(an + 1)\Gamma(bn + 1)}, \quad (2.17)$$

$$B(n) = m\Psi(mn + 1) - \Psi(n + 1) - a\Psi(an + 1) - b\Psi(bn + 1) - \frac{1}{n}, \quad (2.18)$$

and $\Psi(x) = \frac{d}{dx} \log \Gamma(x)$ is the digamma function. Note that the single-log solution given in [20] coincides with (2.15).[‡]

On the other hand, the solutions of the GKZ equation (2.11) associated with fractional $\rho = k_2/a, k_3/b$ are *unphysical*, which must be abandoned because our interest is only in the BPS D-brane system on the non-compact orbifolds.

In fact, the use of the *Meijer G-functions* (see the next section) enables us to study systematically the *closed sub-monodromies* of the three periods $\{1, \hat{U}_1(z), \hat{U}_2(z)\}$ not only around the large radius limit point $z = 0$, but also around the Landau–Ginzburg point $z = \infty$ (hence also around the discriminant locus $z = 1$). However, instead of treating the general orbifold models rather abstractly, we will restrict ourselves below to the three distinguished models, because the connection of them with the local $E_{6,7,8}$ del Pezzo models is very interesting, and that with the $E_{6,7,8}$ tori greatly facilitates the exact analysis of the Picard–Fuchs system of the orbifolds.

2.3 Three distinguished models

The three distinguished orbifolds mentioned in the last paragraph of the preceding subsection are $(m; a, b) = (3; 1, 1), (4; 1, 2)$ and $(6; 2, 3)$, which we call $\mathbf{Z}_3, \mathbf{Z}_4$ and \mathbf{Z}_6 models for simplicity.

For these models, it is possible to factorize an appropriate Picard–Fuchs operator of rank three \mathcal{L}_{orb} on the right of the GKZ operator \square_{orb} , the three solutions of which close under the monodromy actions and indeed correspond to the zero, two- and four-cycles on the exceptional divisor. In fact, the GKZ operators (2.11) of $\mathbf{Z}_3, \mathbf{Z}_4$ and \mathbf{Z}_6 models

[‡]The factor $(Nln + 1)!$ in (28) of [20] should read $(Nln - 1)!$.

admit respectively the following factorizations:

$$\square_{\text{orb}} = \left\{ \Theta_z^2 - z \left(\Theta_z + \frac{1}{3} \right) \left(\Theta_z + \frac{2}{3} \right) \right\} \circ \Theta_z, \quad (2.19)$$

$$\square_{\text{orb}} = \left(\Theta_z - \frac{1}{2} \right) \circ \left\{ \Theta_z^2 - z \left(\Theta_z + \frac{1}{4} \right) \left(\Theta_z + \frac{3}{4} \right) \right\} \circ \Theta_z, \quad (2.20)$$

$$\square_{\text{orb}} = \left(\Theta_z - \frac{1}{3} \right) \left(\Theta_z - \frac{1}{2} \right) \left(\Theta_z - \frac{2}{3} \right) \circ \left\{ \Theta_z^2 - z \left(\Theta_z + \frac{1}{6} \right) \left(\Theta_z + \frac{5}{6} \right) \right\} \circ \Theta_z. \quad (2.21)$$

Hence we can define the Picard–Fuchs operator by

$$\mathcal{L}_{\text{orb}} = \mathcal{L}_{\text{ell}} \circ \Theta_z = \left\{ \Theta_z^2 - z(\Theta_z + \alpha_1)(\Theta_z + \alpha_2) \right\} \circ \Theta_z, \quad (2.22)$$

where $(\alpha_1, \alpha_2) = (\frac{1}{3}, \frac{2}{3}), (\frac{1}{4}, \frac{3}{4}), (\frac{1}{6}, \frac{5}{6})$, for $\mathbf{Z}_3, \mathbf{Z}_4, \mathbf{Z}_6$ orbifold model respectively, and \mathcal{L}_{ell} is the Picard–Fuchs operator of the torus which shares the same toric data (2.4) with the corresponding orbifold, but has the different ansatz: $\Pi(a_i) = f(z)/a_0$ for its periods.

2.4 Picard–Fuchs equations for local del Pezzo models

In this subsection, we collect the facts about the toric description of the three local del Pezzo models and their Picard–Fuchs equations [21, 22], which are closely related to those of the three orbifold models described in the previous subsection, for convenience.

$E_{6,7,8}$ del Pezzo surfaces $S_{6,7,8}$ can be realized as the hypersurfaces in weighted projective threefolds:

$$E_6 : \mathbf{P}(1, 1, 1, 1)[3], \quad (2.23)$$

$$E_7 : \mathbf{P}(1, 1, 1, 2)[4], \quad (2.24)$$

$$E_8 : \mathbf{P}(1, 1, 2, 3)[6]. \quad (2.25)$$

If one of them, which we denote by S_N , $N = 6, 7, 8$, is embedded in a compact Calabi–Yau threefold X , then the neighborhood of S_N in X is identified with the canonical line bundle of S_N : $K_{S_N} \cong \mathcal{O}_{S_N}(-1)$, where the right hand side is the restriction to the hypersurface S_N of the orbifold line bundle $\mathcal{O}_{\mathbf{P}(1,1,a,b)}(-1)$ on the weighted projective threespace with $(a, b) = (1, 1), (1, 2), (2, 3)$ for $N = 6, 7, 8$ respectively.

The triple intersection of the E_N del Pezzo surface S_N embedded in a Calabi–Yau threefold X is computed as

$$S_N \cdot S_N \cdot S_N = c_1(S_N) \cdot c_1(S_N) = 9 - N. \quad (2.26)$$

We see that the non-compact toric Calabi–Yau fivefold associated with the local del Pezzo model is the rank two orbifold bundle on $\mathbf{P} := \mathbf{P}(1, 1, a, b)$:

$$\mathcal{O}_{\mathbf{P}}(-m) \oplus \mathcal{O}_{\mathbf{P}}(-1). \quad (2.27)$$

In fact, this toric data is shared with both the $E_{6,7,8}$ torus and the $\mathbf{Z}_{3,4,6}$ blown-up orbifold model, because the former can be realized as a complete intersection $\mathbf{P}(1, 1, a, b)[1, m]$ and the exceptional divisor of the latter as a hypersurface $\mathbf{P}(1, 1, a, b)[1]$.

A realization of (2.27) by means of the homogeneous coordinates, the first two of which represent the non-compact directions, becomes

$$(x_{-1}, x_0; x_1, x_2, x_3, x_4) \sim (\lambda^{-1} x_{-1}, \lambda^{-m} x_0; \lambda x_1, \lambda x_2, \lambda^a x_3, \lambda^b x_4), \quad (2.28)$$

from which we identify the Mori vector as $l = (-1, -m; 1, 1, a, b)$, that is,

$$E_6 : l = (-1, -3; 1, 1, 1, 1), \quad (2.29)$$

$$E_7 : l = (-1, -4; 1, 1, 1, 2), \quad (2.30)$$

$$E_8 : l = (-1, -6; 1, 1, 2, 3). \quad (2.31)$$

The formula of the GKZ operator for a given Mori vector l (2.10) gives the GKZ equation for the local del Pezzo models under the ansatz for the periods $\Pi(a_i) = f(z)/a_0$:

$$\square_{\text{dP}} = \Theta_z \circ \square_{\text{orb}}, \quad (2.32)$$

where the $E_{6,7,8}$ del Pezzo models correspond to the $\mathbf{Z}_{3,4,6}$ orbifold models respectively. Note that the GKZ equations for the $E_{6,7,8}$ torus and the $\mathbf{Z}_{3,4,6}$ orbifold model can be obtained if we take $\Pi(a_i) = f(z)/(a_{-1}a_0)$ and $\Pi(a_i) = f(z)/a_{-1}$ for the periods respectively.

To summarize, the relations among the Picard–Fuchs operators of $\mathbf{Z}_{3,4,6}$ orbifolds, $E_{6,7,8}$ del Pezzo surfaces and $E_{6,7,8}$ tori become

$$\mathcal{L}_{\text{dP}} = \mathcal{L}_{\text{orb}} = \mathcal{L}_{\text{ell}} \circ \Theta_z = \left\{ \Theta_z^2 - z(\Theta_z + \alpha_1)(\Theta_z + \alpha_2) \right\} \circ \Theta_z, \quad (2.33)$$

where (α_1, α_2) takes

$$(\alpha_1, \alpha_2) = \left(\frac{1}{3}, \frac{2}{3} \right), \quad \left(\frac{1}{4}, \frac{3}{4} \right), \quad \left(\frac{1}{6}, \frac{5}{6} \right) \quad (2.34)$$

for the $\mathbf{Z}_{3,4,6}$ (or $E_{6,7,8}$) models respectively.

3 Solutions of Picard–Fuchs equations

The Picard–Fuchs equations $\mathcal{L}_{\text{ell}} \circ \Theta_z \Pi = 0$ have already appeared in the literature [3, 14, 19, 21, 22, 23, 24] in the context of local mirror symmetry and D-brane physics. Since the Picard–Fuchs operator has the factorized form $\mathcal{L}_{\text{ell}} \circ \Theta_z$ one may obtain the solution by performing the logarithmic integral of the torus periods $\varpi(z)$ which obey $\mathcal{L}_{\text{ell}} \varpi(z) = 0$. See [24] for a recent thorough treatment along this line in the case of the del Pezzo models. It has been recognized, however, that the method of Meijer G-functions is more systematic in dealing with the generalized hypergeometric equation [23, 7, 8]. In particular, the analytic continuation of periods between a patch $|z| < 1$ (the large radius region) and a patch $|z| > 1$ (the orbifold/Landau-Ginzburg region) can be performed unambiguously. It also turns out that Meijer G-functions provide a suitable set of fundamental solutions in constructing a mirror map as will be observed in section 4. Thus we think of it worth presenting the details of the analysis with the use of Meijer G-functions.

Meijer G-functions are defined by [25]

$$\begin{aligned} & \mathbf{G}_{r+r',s+s'}^{s,r} \left(\begin{array}{cccccc} \rho_1 & \cdots & \rho_r & \rho_{r+1} & \cdots & \rho_{r+r'} \\ \sigma_1 & \cdots & \sigma_s & \sigma_{s+1} & \cdots & \sigma_{s+s'} \end{array} \middle| z \right) \\ &= \int_{\gamma} \frac{ds}{2\pi i} \frac{\Gamma(\sigma_1 - s) \cdots \Gamma(\sigma_s - s) \Gamma(1 - \rho_1 + s) \cdots \Gamma(1 - \rho_r + s)}{\Gamma(\rho_{r+1} - s) \cdots \Gamma(\rho_{r+r'} - s) \Gamma(1 - \sigma_{s+1} + s) \cdots \Gamma(1 - \sigma_{s+s'} + s)} z^s, \end{aligned} \quad (3.1)$$

where the integration path γ runs from $-i\infty$ to $+i\infty$ so as to separate the poles at $s = \sigma_i + n$ from those at $s = -n - 1 + \rho_i$ with n being the non-negative integers. They satisfy the linear differential equation

$$\left\{ \prod_{i=1}^{s+s'} (\Theta_z - \sigma_i) - (-1)^\mu z \prod_{j=1}^{r+r'} (\Theta_z - \rho_j + 1) \right\} \mathbf{G} = 0, \quad (3.2)$$

where $\mu = r' - s \pmod{2}$.

Let us set $r + r' = s + s' = 3$ and $\rho_1 = \alpha_1$, $\rho_2 = \alpha_2$, $\rho_3 = 1$, $\sigma_i = 0$, then (3.2) is reduced to our Picard–Fuchs equations with (2.33) which have the regular singular points at $z = 0, 1$ and ∞ . It is known that a fundamental system of solutions around $z = 0$ as well as $z = \infty$ is given by Meijer G-functions [25]. For these regions, thus, solutions to

$\mathcal{L}_{\text{ell}} \circ \Theta_z \Pi = 0$ are derived from Meijer G-functions

$$\mathbf{G}_{3,3}^{s,r} \left(\begin{matrix} \alpha_1 & \alpha_2 & 1 \\ 0 & 0 & 0 \end{matrix} \middle| (-1)^\mu z \right). \quad (3.3)$$

As a fundamental system of solutions we take $(1, U_1(z), U_2(z))$ where

$$\begin{aligned} U_1(z) &= -\frac{\sin \pi \alpha_1}{\pi} \mathbf{G}_{3,3}^{2,2} \left(\begin{matrix} \alpha_1 & \alpha_2 & 1 \\ 0 & 0 & 0 \end{matrix} \middle| -z \right) \\ &= -\frac{\sin \pi \alpha_1}{2\pi^2 i} \int_{\gamma} ds \frac{\Gamma(\alpha_1 + s) \Gamma(\alpha_2 + s) \Gamma(-s)^2}{\Gamma(1-s) \Gamma(1+s)} (-z)^s, \end{aligned} \quad (3.4)$$

$$\begin{aligned} U_2(z) &= -\frac{\sin \pi \alpha_1}{\pi} \mathbf{G}_{3,3}^{3,2} \left(\begin{matrix} \alpha_1 & \alpha_2 & 1 \\ 0 & 0 & 0 \end{matrix} \middle| z \right) \\ &= -\frac{\sin \pi \alpha_1}{2\pi^2 i} \int_{\gamma} ds \frac{\Gamma(\alpha_1 + s) \Gamma(\alpha_2 + s) \Gamma(-s)^3}{\Gamma(1-s)} z^s. \end{aligned} \quad (3.5)$$

Here a normalization factor $-\sin \pi \alpha_1 / \pi$, which equals $-1 / \Gamma(\alpha_1) \Gamma(\alpha_2)$, has been introduced for convenience. The path γ is depicted in Fig.1. Examining the asymptotic

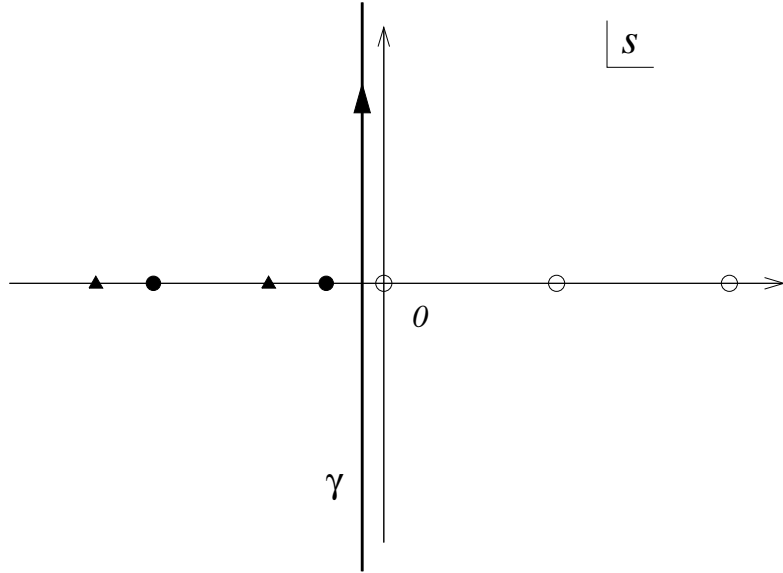


Figure 1: The integration path γ for $\mathbf{G}_{3,3}^{2,2}$ and $\mathbf{G}_{3,3}^{3,2}$.

behavior of integrands as $s \rightarrow \pm i\infty$ with the aid of Stirling's formula, it is shown that the integrals converge if $|\arg(-z)| < \pi$ for $U_1(z)$ and $|\arg(z)| < 2\pi$ for $U_2(z)$. In the

following we choose a branch so that

$$\log(-z) = \log(z) + i\pi. \quad (3.6)$$

3.1 Solutions at $z = 0$

When $|z| < 1$, we can close the contour γ to the right and evaluate the integrals as a sum over the residues of poles at $s = 0, 1, 2, \dots$. As a result we obtain

$$U_1(z) = \log\left(\frac{-z}{e^\beta}\right) + \sum_{n=1}^{\infty} A(n)z^n, \quad (3.7)$$

$$U_2(z) = -\frac{1}{2}\log^2\left(\frac{z}{e^\beta}\right) - \sum_{n=1}^{\infty} A(n)z^n \log\left(\frac{z}{e^\beta}\right) - \sum_{n=1}^{\infty} A(n)B(n)z^n - \xi, \quad (3.8)$$

where

$$\begin{aligned} A(n) &= \frac{(\alpha_1)_n(\alpha_2)_n}{(n!)^2 n}, \\ B(n) &= \sum_{k=0}^{n-1} \left(\frac{1}{k + \alpha_1} + \frac{1}{k + \alpha_2} - \frac{2}{k + 1} \right) - \frac{1}{n}, \end{aligned} \quad (3.9)$$

and $(\alpha)_n = \Gamma(\alpha + n)/\Gamma(\alpha)$. Here two constants β and ξ are given by

$$\begin{aligned} \beta &= -\Psi(\alpha_1) - \Psi(\alpha_2) + 2\Psi(1), \\ \xi &= \frac{1}{2}(\Psi'(\alpha_1) + \Psi'(\alpha_2) + 2\Psi'(1)). \end{aligned} \quad (3.10)$$

From the special values of $\Psi(x)$ one can check that $e^\beta = \prod_i |l_i^{-l_i}|$ (as defined in (2.9)) = $\{27, 64, 432\}$ and $\xi = \pi^2/6 \times \{5, 7, 13\}$ for (α_1, α_2) given in (2.34). For later use, we note the relation

$$U_2(z) = -\frac{1}{2}U_1^2(z) + \pi i U_1(z) + \frac{\pi^2}{2} - \xi + O(z). \quad (3.11)$$

Under $z \rightarrow e^{2\pi i} z$, the monodromy matrix acting on the basis

$$\Pi_U = \left(1, \frac{U_1(z)}{2\pi i}, -\frac{U_2(z)}{(2\pi i)^2} \right) \quad (3.12)$$

is obtained as

$$M_0 = \begin{pmatrix} 1 & 0 & 0 \\ 1 & 1 & 0 \\ 0 & 1 & 1 \end{pmatrix} \quad (3.13)$$

irrespective of the models.

3.2 Solutions at $z = \infty$

For $|z| > 1$ the contour γ can be closed to the left. Then, summing over the residues of poles at $s = -\alpha_i - n$ with non-negative integers n we have power series expansions which are expressed in terms of generalized hypergeometric functions

$$\begin{pmatrix} U_1^\infty(\zeta) \\ U_2^\infty(\zeta) \end{pmatrix} = - \begin{pmatrix} Y_{11} & Y_{12} \\ Y_{21} & Y_{22} \end{pmatrix} \begin{pmatrix} \zeta^{\alpha_1} {}_3F_2(\alpha_1, \alpha_1, \alpha_1; 1 + \alpha_1, 2\alpha_1; \zeta) \\ \zeta^{\alpha_2} {}_3F_2(\alpha_2, \alpha_2, \alpha_2; 1 + \alpha_2, 2\alpha_2; \zeta) \end{pmatrix}, \quad (3.14)$$

where $\zeta = 1/z$ and

$$\begin{aligned} Y_{11} &= \frac{e^{-i\pi\alpha_1} \Gamma(\alpha_2 - \alpha_1)}{\alpha_1 \Gamma(\alpha_2)^2}, & Y_{12} &= Y_{11}(\alpha_1 \leftrightarrow \alpha_2), \\ Y_{21} &= \frac{\Gamma(\alpha_1) \Gamma(\alpha_2 - \alpha_1)}{\alpha_1 \Gamma(\alpha_2)}, & Y_{22} &= Y_{21}(\alpha_1 \leftrightarrow \alpha_2). \end{aligned} \quad (3.15)$$

It is easy to see how these solutions are related to Meijer G-functions. Upon a change of variable $z = 1/\zeta$ (2.33) takes again the Meijer form

$$\{(\Theta_\zeta - \alpha_1)(\Theta_\zeta - \alpha_2)\Theta_\zeta - \zeta\Theta_\zeta^3\} f = 0 \quad (3.16)$$

whose solutions are given by

$$G_{3,3}^{s,r} \left(\begin{matrix} 1 & 1 & 1 \\ \alpha_1 & \alpha_2 & 0 \end{matrix} \middle| (-1)^{s+r+1} \zeta \right). \quad (3.17)$$

Setting $(s, r) = (2, 2)$ and $(3, 2)$ we find

$$\begin{aligned} U_1^\infty(\zeta) &= -\frac{\sin \pi\alpha_1}{\pi} G_{3,3}^{2,2} \left(\begin{matrix} 1 & 1 & 1 \\ \alpha_1 & \alpha_2 & 0 \end{matrix} \middle| -\zeta \right), \\ U_2^\infty(\zeta) &= -\frac{\sin \pi\alpha_1}{\pi} G_{3,3}^{3,2} \left(\begin{matrix} 1 & 1 & 1 \\ \alpha_1 & \alpha_2 & 0 \end{matrix} \middle| \zeta \right). \end{aligned} \quad (3.18)$$

The monodromy matrix at $z = \infty$ is now evaluated to be

$$M_\infty = \begin{pmatrix} 1 & 0 & 0 \\ 0 & 1 - \lambda & -\lambda \\ 0 & 1 & 1 \end{pmatrix}, \quad (3.19)$$

where $\lambda = 4 \sin^2 \pi\alpha_1 = 3, 2, 1$ and $(M_\infty)^m = I$ with $m = 3, 4, 6$ for (α_1, α_2) in (2.34). Thus \mathcal{Z}_m quantum symmetries are realized at the $z = \infty$ orbifold/Landau–Ginzburg points.

Now that monodromies at $z = 0$ and $z = \infty$ have been determined, one may infer the monodromy matrix M_1 at $z = 1$ from the relation $M_1 M_0 = M_\infty$,

$$M_1 = M_\infty M_0^{-1} = \begin{pmatrix} 1 & 0 & 0 \\ -1 & 1 & -\lambda \\ 0 & 0 & 1 \end{pmatrix}. \quad (3.20)$$

In the next section, we confirm this by explicitly constructing solutions at $z = 1$.

3.3 Solutions at $z = 1$

In contrast to the previous cases, solutions of $\mathcal{L}_{\text{ell}} \circ \Theta_z \Pi = 0$ around $z = 1$ cannot be expressed in the form of Meijer G-functions. In fact, the Picard–Fuchs operators (2.33) do not take the Meijer form for the variable $u = 1 - z$. Thus, in subsection 3.3.1, we first solve the differential equation recursively, and then, in subsection 3.3.2, we give a method to construct solutions by the logarithmic integral of corresponding torus periods which are given by Meijer G-functions.

3.3.1 Solutions from the recursion relation

Making a change of variable $u = 1 - z$, we rewrite the Picard–Fuchs equations as

$$\left\{ \Theta_u^3 + \frac{u+2}{u-1} \Theta_u^2 + \frac{\alpha_1 \alpha_2 u^2 - \alpha_1 \alpha_2 u + 1}{(u-1)^2} \Theta_u \right\} \Pi = 0. \quad (3.21)$$

If we set $\Pi = \sum_{n=0}^{\infty} a_n u^{n+\rho}$, the indicial equation reads $\rho(\rho-1)^2 = 0$. Thus we have a set of solutions $(1, V_1(u), V_2(u))$,

$$V_1(u) = \sum_{n=0}^{\infty} a_n u^{n+1}, \quad a_0 = 1, \quad (3.22)$$

$$V_2(u) = V_1(u) \log u + \sum_{n=1}^{\infty} b_n u^{n+1}, \quad (3.23)$$

where the coefficients a_n and b_n can be determined recursively.

The recursion relations for the coefficients a_n in V_1 are

$$a_1 = \frac{1}{2}(1 + \alpha_1 \alpha_2), \quad (3.24)$$

$$\begin{aligned} m(m + \alpha_1)(m + \alpha_2)a_{m-1} + (m + 1)\{-2(m + 1)^2 + (m + 1) - \alpha_1 \alpha_2\}a_m \\ + (m + 2)(m + 1)^2 a_{m+1} = 0, \quad \text{for } m \geq 1. \end{aligned} \quad (3.25)$$

The recursion relations obeyed by b_n in V_2 are

$$-(4 + \alpha_1\alpha_2)a_0 + 5a_1 + 2b_1 = 0, \quad (3.26)$$

$$(5 + \alpha_1\alpha_2)a_0 - (20 + \alpha_1\alpha_2)a_1 + 16a_2 - (12 + 2\alpha_1\alpha_2)b_1 + 12b_2 = 0, \quad (3.27)$$

$$\begin{aligned} & \{3m^2 + 2m + \alpha_1\alpha_2\}a_{m-1} - \{6(m+1)^2 - 2(m+1) + \alpha_1\alpha_2\}a_m \\ & + (3m+5)(m+1)a_{m+1} + m(m+\alpha_1)(m+\alpha_2)b_{m-1} \\ & - (m+1)\{2(m+1)^2 - (m+1) + \alpha_1\alpha_2\}b_m \\ & + (m+2)(m+1)^2b_{m+1} = 0, \quad \text{for } m \geq 2. \end{aligned} \quad (3.28)$$

Consequently we obtain the following expressions for $(\alpha_1, \alpha_2) = (\frac{1}{3}, \frac{2}{3})$,

$$V_1(u) = u + \frac{11}{18}u^2 + \frac{109}{243}u^3 + \frac{9389}{26244}u^4 + \dots, \quad (3.29)$$

$$V_2(u) = V_1(u) \log u + \frac{7}{12}u^2 + \frac{877}{1458}u^3 + \frac{176015}{314928}u^4 + \dots. \quad (3.30)$$

For $(\alpha_1, \alpha_2) = (\frac{1}{4}, \frac{3}{4})$ we have

$$V_1(u) = u + \frac{19}{32}u^2 + \frac{1321}{3072}u^3 + \frac{22291}{65536}u^4 + \dots, \quad (3.31)$$

$$V_2(u) = V_1(u) \log u + \frac{39}{64}u^2 + \frac{5729}{9216}u^3 + \frac{451495}{786432}u^4 + \dots. \quad (3.32)$$

For $(\alpha_1, \alpha_2) = (\frac{1}{6}, \frac{5}{6})$ we get

$$V_1(u) = u + \frac{41}{72}u^2 + \frac{6289}{15552}u^3 + \frac{2122721}{6718464}u^4 + \dots, \quad (3.33)$$

$$V_2(u) = V_1(u) \log u + \frac{31}{48}u^2 + \frac{30281}{46656}u^3 + \frac{47918861}{80621568}u^4 + \dots. \quad (3.34)$$

3.3.2 Torus periods

Let us now examine torus periods to find the closed form of $V_1(u)$ and $V_2(u)$. The Picard–Fuchs equations for the torus periods are

$$\mathcal{L}_{\text{ell}} \Pi_{\text{torus}} = \left\{ \Theta_z^2 - z(\Theta_z + \alpha_1)(\Theta_z + \alpha_2) \right\} \Pi_{\text{torus}} = 0 \quad (3.35)$$

whose solutions are given by Meijer G-functions

$$\varpi_0(z) = \frac{\sin \pi \alpha_1}{\pi} G_{2,2}^{1,2} \left(\begin{matrix} \alpha_1 & \alpha_2 \\ 0 & 0 \end{matrix} \middle| -z \right), \quad (3.36)$$

$$\varpi_1(z) = \frac{\sin \pi \alpha_1}{\pi} G_{2,2}^{2,2} \left(\begin{matrix} \alpha_1 & \alpha_2 \\ 0 & 0 \end{matrix} \middle| z \right). \quad (3.37)$$

Proceeding in parallel with sections 3.1 and 3.2 we first obtain the solutions at $z = 0$

$$\varpi_0(z) = {}_2F_1(\alpha_1, \alpha_2; 1; z), \quad (3.38)$$

$$\varpi_1(z) = -\varpi_0(z) \log \left(\frac{z}{e^\beta} \right) - \sum_{n=1}^{\infty} n A(n) \left(B(n) + \frac{1}{n} \right) z^n. \quad (3.39)$$

The solutions at $z = \infty$ turn out to be

$$\begin{pmatrix} \varpi_0^\infty(\zeta) \\ \varpi_1^\infty(\zeta) \end{pmatrix} = \begin{pmatrix} X_{11} & X_{12} \\ X_{21} & X_{22} \end{pmatrix} \begin{pmatrix} \zeta^{\alpha_1} {}_2F_1(\alpha_1, \alpha_1; 2\alpha_1; \zeta) \\ \zeta^{\alpha_2} {}_2F_1(\alpha_2, \alpha_2; 2\alpha_2; \zeta) \end{pmatrix}, \quad (3.40)$$

where $\zeta = 1/z$ and

$$\begin{aligned} X_{11} &= \frac{e^{-i\pi\alpha_1} \Gamma(\alpha_2 - \alpha_1)}{\Gamma(\alpha_2)^2}, & X_{12} &= X_{11}(\alpha_1 \leftrightarrow \alpha_2), \\ X_{21} &= \frac{\Gamma(\alpha_1) \Gamma(\alpha_2 - \alpha_1)}{\Gamma(\alpha_2)}, & X_{22} &= X_{21}(\alpha_1 \leftrightarrow \alpha_2). \end{aligned} \quad (3.41)$$

As opposite to the case of orbifold/del Pezzo models, the Picard–Fuchs equation around $z = 1$ takes the same form as the one around $z = 0$

$$\left\{ \Theta_u^2 - u(\Theta_u + \alpha_1)(\Theta_u + \alpha_2) \right\} \Pi_{\text{torus}} = 0, \quad (3.42)$$

where $u = 1 - z$. Hence its solutions are given by $\varpi_0(u)$ and $\varpi_1(u)$. Using the Barnes' Lemma [26, p.289],

$$\begin{aligned} & {}_2F_1(\alpha_1, \alpha_2; 1; z) \\ &= \frac{\sin^2 \pi \alpha_1}{\pi^2} \int_{-i\infty}^{i\infty} \frac{ds}{2\pi i} \int_{-i\infty}^{i\infty} \frac{dt}{2\pi i} \Gamma(\alpha_1 + t) \Gamma(\alpha_2 + t) \Gamma(s - t) \Gamma(-t) \Gamma(-s) (-z)^s \\ &= \frac{\sin^2 \pi \alpha_1}{\pi^2} \int_{-i\infty}^{i\infty} \frac{dt}{2\pi i} \Gamma(\alpha_1 + t) \Gamma(\alpha_2 + t) \Gamma(-t)^2 (1 - z)^t, \quad |\arg(-z)| < \pi, \end{aligned} \quad (3.43)$$

we get the connection formulas for torus periods

$$\varpi_0(z) = \frac{\sin \pi \alpha_1}{\pi} \varpi_1(u), \quad \varpi_1(z) = \frac{\pi}{\sin \pi \alpha_1} \varpi_0(u). \quad (3.44)$$

3.3.3 Solutions based on torus periods

Since $\mathcal{L} = \mathcal{L}_{\text{ell}} \circ \Theta_z$, the orbifold/del Pezzo periods can be obtained as the logarithmic integral of the torus periods. In fact, for $|z| < 1$ they are related through

$$\Theta_z U_1(z) = \varpi_0(z), \quad \Theta_z U_2(z) = \varpi_1(z). \quad (3.45)$$

With the help of this relation and (3.44), $U_i(z)$ can be analytically continued in the patch $|1 - z| < 1$. First we have

$$U_1(z) = -\frac{\sin \pi \alpha_1}{\pi} \int_0^u \frac{du'}{1 - u'} \varpi_1(u') + C_1, \quad (3.46)$$

$$U_2(z) = -\frac{\pi}{\sin \pi \alpha_1} \int_0^u \frac{du'}{1 - u'} \varpi_0(u') + C_2, \quad (3.47)$$

where C_i are integration constants. Then we assume

$$\begin{aligned} U_1(z) &= A_1 V_1(u) + B_1 V_2(u) + C_1, \\ U_2(z) &= A_2 V_1(u) + B_2 V_2(u) + C_2, \end{aligned} \quad (3.48)$$

where $V_i(u)$ have been defined in (3.22), (3.23), and A_i, B_i are connection coefficients. Performing the integrals in (3.46), (3.47) we arrive at

$$V_1(u) = \sum_{k=0}^{\infty} \sum_{n=0}^{\infty} n A(n) \frac{u^{k+n+1}}{k+n+1}, \quad (3.49)$$

$$\begin{aligned} V_2(u) &= V_1(u) \log u \\ &+ \sum_{k=0}^{\infty} \sum_{n=0}^{\infty} n A(n) \left(1 + B(n) + \frac{1}{n} - \frac{1}{k+n+1} \right) \frac{u^{k+n+1}}{k+n+1} \end{aligned} \quad (3.50)$$

which indeed agree with (3.29)–(3.34). We also fix the coefficients A_i, B_i as

$$\begin{aligned} A_1 &= -\frac{\sin \pi \alpha_1}{\pi} (1 + \beta), & B_1 &= \frac{\sin \pi \alpha_1}{\pi}, \\ A_2 &= -\frac{\pi}{\sin \pi \alpha_1}, & B_2 &= 0. \end{aligned} \quad (3.51)$$

Our remaining task is to determine the constants C_i . For this we notice that $U_i(1) = C_i$ and $U_i(1)$ themselves can be determined by $U_i(1) = U_i^\infty(\zeta = 1)$. Eq.(3.45) is rewritten as

$$U_2^\infty(\zeta) = -\int_0^\zeta \frac{d\zeta'}{\zeta'} \varpi_1^\infty(\zeta'), \quad (3.52)$$

where $U_2^\infty(\zeta = 0) = 0$ has been used. Substituting here the analytic continuation formula

$$\frac{\varpi_1^\infty(\zeta)}{\zeta} = \frac{\pi}{\sin \pi \alpha_1} \zeta^{-1+\alpha_1} {}_2F_1(\alpha_1, \alpha_1; 1; 1 - \zeta), \quad (3.53)$$

we evaluate [24]

$$\begin{aligned} C_2 &= -\frac{\pi}{\sin \pi \alpha_1} \int_0^1 d\zeta \zeta^{-1+\alpha_1} {}_2F_1(\alpha_1, \alpha_1; 1; 1 - \zeta) \\ &= -\Gamma(\alpha_2) \sum_{n=0}^{\infty} \frac{\Gamma(\alpha_1 + n)^2}{\Gamma(\alpha_1 + n + 1)n!} \\ &= -\frac{\pi^2}{\sin^2 \pi \alpha_1}. \end{aligned} \quad (3.54)$$

Therefore we find

$$\frac{U_2(1)}{(2\pi i)^2} = \frac{1}{\lambda} \quad (3.55)$$

which will play a role later.

In a similar vein one can determine $C_1 = U_1(1) = U_1^\infty(1)$ as follows [27]

$$\begin{aligned} C_1 &= -\int_0^1 \frac{d\zeta}{\zeta} \varpi_0^\infty(\zeta) \\ &= \frac{i\pi}{\Gamma(\alpha_1)^2 \Gamma(\alpha_2)^2} \int_0^1 \frac{d\zeta}{\zeta} \varpi_1^\infty(\zeta) \\ &\quad - \frac{\cos \pi \alpha_1}{\Gamma(\alpha_1) \Gamma(\alpha_2)} \int_0^1 \frac{d\zeta}{\zeta} \left(X_{21} \zeta^{\alpha_1} {}_2F_1(\alpha_1, \alpha_1; 2\alpha_1; \zeta) - X_{22} \zeta^{\alpha_2} {}_2F_1(\alpha_2, \alpha_2; 2\alpha_2; \zeta) \right). \end{aligned} \quad (3.56)$$

Here the first term has already been evaluated as above, whereas the second term is computed numerically. The results read

$$\frac{C_1}{2\pi i} = \frac{1}{2} + \begin{cases} i 0.462757882001768178 \dots, & \text{for } \mathbf{Z}_3 \text{ (or } E_6), \\ i 0.610262151883452845 \dots, & \text{for } \mathbf{Z}_4 \text{ (or } E_7), \\ i 0.928067181776930407 \dots, & \text{for } \mathbf{Z}_6 \text{ (or } E_8). \end{cases} \quad (3.57)$$

It is now possible to check that the monodromy matrix at $z = 1$ is indeed given by (3.20).

In view of (3.18), remember that C_1 is the value of the Meijer G-function at $\zeta = 1$

$$C_1 = -\frac{\sin \pi \alpha_1}{\pi} G_{3,3}^{2,2} \left(\begin{matrix} 1 & 1 & 1 \\ \alpha_1 & \alpha_2 & 0 \end{matrix} \middle| -1 \right). \quad (3.58)$$

We wish to point out an amazing relationship of the values of C_1 to the special values of zeta functions in number theory. For this let us introduce the Hurwitz zeta function

$$\zeta(s, a) = \sum_{n=0}^{\infty} \frac{1}{(n+a)^s} \quad (3.59)$$

for $a > 0$ [28]. It converges absolutely for $\text{Re } s > 1$ and reduces to the Riemann zeta function for $a = 1$. $\zeta(s, a)$ can be analytically continued over the complex s -plane except for $s = 1$ at which a simple pole appears. We also introduce the Dirichlet L -function

$$L(s, \chi) = \sum_{n=1}^{\infty} \frac{\chi(n)}{n^s}, \quad (3.60)$$

where $\chi(n)$, called the Dirichlet character, obeys $\chi(n+f) = \chi(n)$ with a positive integer f , $\chi(mn) = \chi(m)\chi(n)$ if m and n are prime to f and $\chi(n) = 0$ if n is not prime to f . These two zeta functions are related through

$$L(s, \chi) = f^{-s} \sum_{n=1}^f \chi(n) \zeta\left(s, \frac{n}{f}\right). \quad (3.61)$$

Now, for the \mathbf{Z}_3 (or E_6) model, there exists a remarkable relation proved by Rodriguez Villegas [29]

$$\text{Im} \left(\frac{C_1}{2\pi i} \right) = \frac{9}{2\pi} L'(-1, \chi), \quad (3.62)$$

where $'$ stands for $\frac{d}{ds}$ and $\chi(n)$ has been defined with $f = 3$

$$\chi(n) = \begin{cases} 1, & n = 1 \pmod{3}, \\ -1, & n = 2 \pmod{3}, \\ 0, & n = 3 \pmod{3}. \end{cases} \quad (3.63)$$

Namely the L -function in (3.62) reads

$$L(s, \chi) = 3^{-s} \left(\zeta\left(s, \frac{1}{3}\right) - \zeta\left(s, \frac{2}{3}\right) \right). \quad (3.64)$$

To be convinced, one can check (3.62) numerically by using the software package Maple to compute special values of $\zeta'(s, a)$ and reproduce (3.57). The proof of (3.62) is based on the relation between special values of L -function and the Mahler measure in number theory, which we will discuss further in section 4.4.

For the \mathbf{Z}_4 (or E_7) model, we discover by numerical experiment that

$$\operatorname{Im} \left(\frac{C_1}{2\pi i} \right) = \frac{2}{2\pi} L'(-1, \chi), \quad (3.65)$$

where

$$\chi(n) = \begin{cases} 1, & n = 1, 3 \pmod{8}, \\ -1, & n = 5, 7 \pmod{8}, \\ 0, & n = 2, 4, 6, 8 \pmod{8}, \end{cases} \quad (3.66)$$

and

$$L(s, \chi) = 8^{-s} \left(\zeta\left(s, \frac{1}{8}\right) + \zeta\left(s, \frac{3}{8}\right) - \zeta\left(s, \frac{5}{8}\right) - \zeta\left(s, \frac{7}{8}\right) \right). \quad (3.67)$$

For the \mathbf{Z}_6 (or E_8) model, we find again by experiment that

$$\operatorname{Im} \left(\frac{C_1}{2\pi i} \right) = \frac{10}{2\pi} L'(-1, \chi), \quad (3.68)$$

where

$$\chi(n) = \begin{cases} 1, & n = 1 \pmod{4}, \\ -1, & n = 3 \pmod{4}, \\ 0, & n = 2, 4 \pmod{4}, \end{cases} \quad (3.69)$$

and

$$L(s, \chi) = 4^{-s} \left(\zeta\left(s, \frac{1}{4}\right) - \zeta\left(s, \frac{3}{4}\right) \right). \quad (3.70)$$

In addition it is seen [30] that

$$\operatorname{Im} \left(\frac{C_1}{2\pi i} \right) = \frac{10}{\pi^2} G, \quad (3.71)$$

where G is known as Catalan's constant given by

$$G = \sum_{n=1}^{\infty} \frac{(-1)^{n-1}}{(2n-1)^2} = 0.915965594177 \dots \quad (3.72)$$

Curiously Catalan's constant is ubiquitous in the entropy factors in various mathematical models [30].

Although we shall refrain from describing in detail here, the value of C_1 for the E_5 del Pezzo model is obtained as

$$\frac{C_1}{2\pi i} = \frac{1}{2} + i \frac{4}{2\pi} L'(-1, \chi), \quad (3.73)$$

where $L(s, \chi)$ is given by (3.70) and the expression for $\text{Im}(C_1/2\pi i)$ is due to [29]. We see from (3.68) and (3.73) that

$$\left[\text{Im} \left(\frac{C_1}{2\pi i} \right) \right]_{E_8} / \left[\text{Im} \left(\frac{C_1}{2\pi i} \right) \right]_{E_5} = \frac{5}{2}. \quad (3.74)$$

From the result of [23], on the other hand, this ratio is evaluated as 2.50000 in agreement with ours.

Finally we recall that the value of $\text{Im}(C_1/2\pi i)$ is of particular interest since it gives the exponent which governs the exponential growth of the Gromov–Witten invariants $n(k)$ [31, 27, 23]

$$|n(k)| \sim \frac{e^{2\pi \text{Im}(\frac{C_1}{2\pi i})k}}{k^3 \log^2 k}. \quad (3.75)$$

It is very intriguing that the special values of zeta functions which are peculiar to number theory reveal themselves in the property of a significant set of numbers such as local Gromov–Witten invariants of Fano manifolds.

4 Mirror maps and modular functions

In this section, first we give the definition of the mirror maps for the non-compact Calabi–Yau models, which identifies the periods corresponding to the D2-brane and the D4-brane. The latter receives the quantum corrections due to the open string world-sheet instantons, which is related to the closed string world-sheet instantons [32]. Hence the study of the disc instanton effects on the D4-brane period in our local Calabi–Yau models is reduced to that of the Gromov–Witten invariants (of genus zero), which have already been done in the literature [21, 22].

On the other hand, the mirror maps of the $E_{6,7,8}$ elliptic curves associated with the local Calabi–Yau models can be beautifully described by classical modular functions. Our second aim in this section is then to elucidate the relation between the Gromov–Witten invariants of the local Calabi–Yau models and these modular functions.

Furthermore we find a beautiful link which connects some arithmetic properties of local mirror symmetry with a recent topic in number theory; the Mahler measure and special values of L -functions. Describing this observation is our third aim in this section.

4.1 Mirror maps for local Calabi–Yau

In this subsection we give the mirror map for orbifolds and del Pezzo models. In the discussion of mirror symmetry, it is sometimes convenient to use the *unnormalized* modulus parameter $z_0 := e^{-\beta}z$ instead of z . Let t_b, t be the complexified Kähler parameters of the orbifold and the del Pezzo model. According to [19, 20] and [22], they are given by the solutions of the Picard–Fuchs equation of the forms:

$$2\pi i t_b = \log(z_0) + O(z_0), \quad (4.1)$$

$$2\pi i t = \log(-z_0) + O(-z_0), \quad (4.2)$$

from which we can determine the mirror maps as

$$2\pi i t_b = U_1(e^\beta z_0) - \pi i = \log(z_0) + \sum_{n=1}^{\infty} A(n) (e^\beta z_0)^n, \quad (4.3)$$

$$2\pi i t = U_1(e^\beta z_0) = \log(-z_0) + \sum_{n=1}^{\infty} A(n) (e^\beta z_0)^n, \quad (4.4)$$

that is, $t_b = t - \frac{1}{2}$. We use the notation $t_b = B_b + iJ_b$ and $t = B + iJ$ to show explicitly the physical content of the complexified Kähler parameters. At the orbifold point $z = \infty$, the vanishing of the period $U_1^\infty(\zeta = 0) = 0$ implies

$$B_b + iJ_b = -\frac{1}{2}, \quad (4.5)$$

$$B + iJ = 0, \quad (4.6)$$

which means that at the orbifold point, the orbifold model is described by a non-singular CFT on the type II string world sheet, while the local del Pezzo model by a singular CFT. Note that the complexified Kähler parameter can also be identified with the central charge of the BPS D2-brane wrapping around the fundamental two-cycle [33].

The inversion of the mirror map for the local del Pezzo model (4.2) is given by

$$E_6 : z_0 = -e^{2\pi i t} - 6 e^{2 \cdot 2\pi i t} - 9 e^{3 \cdot 2\pi i t} - 56 e^{4 \cdot 2\pi i t} + \dots, \quad (4.7)$$

$$E_7 : z_0 = -e^{2\pi i t} - 12 e^{2 \cdot 2\pi i t} - 6 e^{3 \cdot 2\pi i t} - 688 e^{4 \cdot 2\pi i t} + \dots, \quad (4.8)$$

$$E_8 : z_0 = -e^{2\pi i t} - 60 e^{2 \cdot 2\pi i t} + 1530 e^{3 \cdot 2\pi i t} - 274160 e^{4 \cdot 2\pi i t} + \dots. \quad (4.9)$$

Next we consider the period which represents the D4-brane, which we denote by t_d and t_{dP} for the orbifold and the local del Pezzo model. In general, all the periods which

have $\log^2(z_0)$ with an appropriate coefficient as the leading term of the large radius limit $z_0 \rightarrow 0$ can be called the D4-brane, that is, the definition of the D4-brane period has an ambiguity of addition of lower dimensional brane charges [33]. However, we can uniquely determine t_b and t_{dP} by imposing reasonable conditions on them. For the orbifold model, we require that t_d should vanish at the conifold point $z = 1$ [3], from which t_d is fixed up to the normalization. For the local del Pezzo model, on the other hand, it turns out that t_{dP} should vanish at the orbifold point $z = \infty$ [22], which leaves the ambiguity of the addition of t to t_{dP} . However the form of the central charge at the large radius region can be used to fix it. Finally the normalization factors for the D4-branes t_d, t_{dP} can be determined by the volume of the twofolds associated with the local Calabi–Yau models, which we leave to the next section. Thus we arrive at the following results for the *unnormalized* D4-brane periods:

$$t_d = -\frac{U_2(z)}{(2\pi i)^2} + \frac{1}{\lambda}, \quad (4.10)$$

$$t_{dP} = -\frac{U_2(z)}{(2\pi i)^2}. \quad (4.11)$$

Notice that for the local del Pezzo case, *D2- and D4-brane periods are given essentially by the Meijer G-functions.*

In the large radius region $|z| < 1$ of the orbifold model we obtain

$$\begin{aligned} t_d &= \frac{t_b^2}{2} + \frac{1}{(2\pi i)^2} \left(\frac{\pi^2}{2} - \xi \right) + \frac{1}{\lambda} + \mathcal{O}(e^{2\pi i t_b}) \\ &= \frac{t_b^2}{2} + \frac{a + b + ab}{24} + \mathcal{O}(e^{2\pi i t_b}) \end{aligned} \quad (4.12)$$

corresponding to the exceptional divisor $\mathbf{P}(1, a, b)$ in the $\mathbf{C}^3/\mathbf{Z}_m$ model. In the $E_{N=6,7,8}$ del Pezzo model, on the other hand, it follows that

$$t_{dP} = \frac{t^2}{2} - \frac{t}{2} + \frac{1}{12} \frac{3 - N}{9 - N} + \mathcal{O}(e^{2\pi i t}), \quad (4.13)$$

respectively [24].

4.2 Mirror map for tori

The mirror map of the torus is

$$2\pi i \tau = -\frac{\varpi_1(z)}{\varpi_0(z)}, \quad (4.14)$$

where τ is the Kähler modulus parameter of the torus. Using the relation (3.45) we can show that

$$\tau = \frac{dt_{dP}}{dt} = t - \frac{1}{2} + O(e^{2\pi it}), \quad (4.15)$$

which will play an important role in the investigation of the Gromov–Witten invariants in the later subsection.

The inversion of the mirror map for z_0 has the following expansion with $q = e^{2\pi i\tau}$:

$$E_6 : z_0 = q - 15 q^2 + 171 q^3 - 1679 q^4 + 15054 q^5 + \dots, \quad (4.16)$$

$$E_7 : z_0 = q - 40 q^2 + 1324 q^3 - 39872 q^4 + 1136334 q^5 + \dots, \quad (4.17)$$

$$E_8 : z_0 = q - 312 q^2 + 87084 q^3 - 23067968 q^4 + 5930898126 q^5 + \dots. \quad (4.18)$$

There is an efficient way to obtain the power series expansions above. First, it is well-known that the inversion of the mirror maps of $E_{6,7}$ tori (4.16), (4.17) can be written by the *Hauptmodul* of the genus zero subgroups $\Gamma_0(3)$, $\Gamma_0(2)$ of the modular group $\Gamma := \text{PSL}(2; \mathbf{Z})$, which are given by the Thompson series $T_{3B}(q)$, $T_{2B}(q)$ [34, 35]; see [36] for notations:

$$E_6 : z_0(q) = \frac{1}{T_{3B}(q) + 27}, \quad T_{3B}(q) = \left(\frac{\eta(q)}{\eta(q^3)} \right)^{12}, \quad (4.19)$$

$$E_7 : z_0(q) = \frac{1}{T_{2B}(q) + 64}, \quad T_{2B}(q) = \left(\frac{\eta(q)}{\eta(q^2)} \right)^{24}, \quad (4.20)$$

where $\eta(q) = q^{\frac{1}{24}} \prod_{n \geq 1} (1 - q^n)$ is the Dedekind eta function. On the other hand, the inversion for the E_8 case (4.18) is given by the formal q -expansion of the function

$$E_8 : z_0(q) = \frac{2}{j(q) + \sqrt{j(q)(j(q) - 1728)}}, \quad (4.21)$$

where $j(q)$ is the j -invariant defined by

$$j(q) = \frac{E_4(q)^3}{\eta(q)^{24}} = \frac{1}{q} + 744 + 196884 q + 21493760 q^2 + 864299970 q^3 + \dots. \quad (4.22)$$

Here $E_4(q)$ is the Eisenstein series of weight four, also known as the theta function of the E_8 lattice

$$E_4(q) = \left(2 \frac{\eta(q^2)^2}{\eta(q)} \right)^8 + \left(\frac{\eta(q)^2}{\eta(q^2)} \right)^8 = 1 + 240 \sum_{n=1}^{\infty} n^3 \frac{q^n}{1 - q^n}. \quad (4.23)$$

We note that (4.21) has the following integral representation

$$E_8 : \quad z_0(q) = \int_0^q \frac{dq'}{q'} \frac{E_4(q')^{\frac{1}{2}}}{j(q')}. \quad (4.24)$$

Curiously, the following combinations, which can be expressed by the Hauptmodul of the genus zero subgroups $\Gamma_0(3)_+$, $\Gamma_0(2)_+$ and Γ of $\mathrm{PSL}(2; \mathbf{R})$,

$$E_6 : \quad z_0(1 - 27z_0) = \frac{1}{T_{3A}(q) + 36}, \quad (4.25)$$

$$E_7 : \quad z_0(1 - 64z_0) = \frac{1}{T_{2A}(q) + 96}, \quad (4.26)$$

$$E_8 : \quad z_0(1 - 432z_0) = \frac{1}{j(q)}, \quad (4.27)$$

coincide with the inversions of the mirror maps of the one-parameter family of K3 surfaces: $\mathbf{P}^4[2, 3]$, $\mathbf{P}^3[4]$ and $\mathbf{P}(1, 1, 1, 3)[6]$ respectively. The fundamental period ϖ_0 of the torus can be written by the modular functions as

$$E_6 : \varpi_0 = \frac{(T_{3B}(q) + 27)^{\frac{1}{3}}}{T_{3B}(q)^{\frac{1}{4}}} \eta(q)^2 = 1 + 6q + 6q^3 + 6q^4 + 12q^7 + \dots, \quad (4.28)$$

$$E_7 : \varpi_0 = \frac{(T_{2B}(q) + 64)^{\frac{1}{4}}}{T_{2B}(q)^{\frac{1}{6}}} \eta(q)^2 = 1 + 12q - 60q^2 + 768q^3 - 11004q^4 + \dots, \quad (4.29)$$

$$E_8 : \varpi_0 = E_4(q)^{\frac{1}{4}} = 1 + 60q - 4860q^2 + 660480q^3 - 105063420q^4 + \dots. \quad (4.30)$$

4.3 Gromov–Witten invariants

We begin with the Abel–Liouville theorem [37], which states that for the basis $\{\varpi_0, \varpi_1\}$ of the solutions of the Picard–Fuchs equation of the $E_{6,7,8}$ tori (3.35):

$$-\varpi_0(z)\Theta_z\varpi_1(z) + \varpi_1(z)\Theta_z\varpi_0(z) = \frac{1}{1-z}. \quad (4.31)$$

Using the mirror map of the torus (4.14), we can recast this equation as [38, Prop. 4.4] [§]

$$2\pi i \Theta_z \tau = \frac{1}{(1-z)\varpi_0(z)^2}, \quad (4.32)$$

[§]We note that analogous relations hold in the Seiberg–Witten theory for $\mathcal{N} = 2$ $\mathrm{SU}(2)$ Yang–Mills theory with massless fundamental matters [39, eq.(2.16)].

the left hand side of which becomes using (3.45) and (4.15)

$$2\pi iz \frac{d\tau}{dz} = 2\pi i \Theta_z t \frac{d\tau}{dt} = \varpi_0(z) \frac{d\tau}{dt} = \varpi_0(z) \frac{d^2 t_{dP}}{dt^2}. \quad (4.33)$$

Therefore we have the equation for the *unnormalized Yukawa coupling* Y_{ttt}

$$Y_{ttt} := \frac{d^2 t_{dP}}{dt^2} = \frac{1}{(1-z) \varpi_0(z)^3} = \frac{1}{(1-z) {}_2F_1(\alpha_1, \alpha_2; 1; z)^3}. \quad (4.34)$$

The Yukawa coupling Y_{ttt} may admit two expansions according to the two definitions of the mirror maps for the orbifolds and del Pezzos:

$$Y_{ttt} = 1 - \sum_{k=1}^{\infty} n(k) k^3 \frac{e^{2\pi i k t}}{1 - e^{2\pi i k t}} \quad (4.35)$$

$$= 1 - \sum_{k=1}^{\infty} n_b(k) k^3 \frac{e^{2\pi i k t_b}}{1 - e^{2\pi i k t_b}}. \quad (4.36)$$

Since $e^{2\pi i t_b} = -e^{2\pi i t}$, the expansion coefficients, which we call the unnormalized Gromov–Witten invariants, in (4.35) and (4.36) are related via

$$\begin{aligned} n_b(2k+1) &= -n(2k+1), \\ n_b(4k) &= n(4k), \\ n_b(4k+2) &= n(4k+2) + \frac{1}{4} n(2k+1). \end{aligned} \quad (4.37)$$

This phenomenon was first observed in the relation between the Gromov–Witten invariants of the E_5 del Pezzo surface and the Hirzebruch surface \mathbf{F}_0 [22]; both models share the Picard–Fuchs operator $\mathcal{L}_{\text{PF}} = \{\Theta_z^2 - z(\Theta_z + 1/2)^2\} \circ \Theta_z$, but the definitions of the mirror map are different just as in our case of the del Pezzo surfaces and orbifolds.

In terms of the Gromov–Witten invariants, the modulus of the torus can be expressed by those of the corresponding local Calabi–Yau models as

$$q = -e^{2\pi i t} \prod_{k=1}^{\infty} (1 - e^{2\pi i k t})^{k^2 n(k)}, \quad (4.38)$$

$$= e^{2\pi i t_b} \prod_{k=1}^{\infty} (1 - e^{2\pi i k t_b})^{k^2 n_b(k)}. \quad (4.39)$$

On the other hand, from (4.32) $t_b = t - 1/2$ can be obtained as the indefinite logarithmic integration over a combination of the modular functions described in the previous

k	E_6	E_7	E_8
1	9	28	252
2	-18	-136	-9252
3	81	1620	848628
4	-576	-29216	-114265008
5	5085	651920	18958064400
6	-51192	-16627608	-3589587111852
7	565362	465215604	744530011302420
8	-6684480	-13927814272	-165076694998001856
9	83246697	439084931544	38512679141944848024
10	-1080036450	-14417814260960	-9353163584375938364400
11	14483807811	489270286160612	2346467355966572489025540
12	-199613140560	-17060721785061984	-604657435721239536237491472

Table 1: Gromov–Witten invariants $n(k)$

subsection:

$$2\pi it_b = \int \frac{dq'}{q'} (1 - z(q')) \varpi_0(z(q'))^3. \quad (4.40)$$

Explicitly, we have

$$E_6 : e^{2\pi it_b} = q - 9q^2 + 54q^3 - 246q^4 + 909q^5 - 2808q^6 + \dots, \quad (4.41)$$

$$E_7 : e^{2\pi it_b} = q - 28q^2 + 646q^3 - 13768q^4 + 284369q^5 - 5812884q^6 + \dots, \quad (4.42)$$

$$E_8 : e^{2\pi it_b} = q - 252q^2 + 58374q^3 - 13135368q^4 + 2923010001q^5 + \dots. \quad (4.43)$$

Comparison of the inversion of these power series and (4.39) tells us the invariants $\{n_b(k)\}$ and $\{n(k)\}$. The first few values of $n(k)$ may be found, for example, in [24], and are listed in Table 1.

4.4 Local mirror from Mahler measure

Let $P \in \mathbf{C}[x_1^\pm, \dots, x_n^\pm]$ be a Laurent polynomial in n variables. The *logarithmic Mahler measure* of P [40, 30, 29] is defined by

$$m(P) = \frac{1}{(2\pi i)^n} \int_{\mathbf{T}} \log |P(x_1, \dots, x_n)| \frac{dx_1}{x_1} \dots \frac{dx_n}{x_n}, \quad (4.44)$$

where $\mathbf{T} = \{|x_1| = \dots = |x_n| = 1\}$ is the standard torus. If we denote by $\langle P \rangle_0$ the constant term in P , then we have

$$\langle P \rangle_0 = \frac{1}{(2\pi i)^n} \int_{\mathbf{T}} P(x_1, \dots, x_n) \frac{dx_1}{x_1} \dots \frac{dx_n}{x_n}, \quad (4.45)$$

which yields the useful expression for the Mahler measure:

$$m(P) = \operatorname{Re} \left\{ \left\langle \log(P) \right\rangle_0 \right\}. \quad (4.46)$$

Let us consider the Mahler measure of the one-parameter family of polynomials in two variables P_ψ , which represents the local mirror geometry of the torus model:

$$\begin{aligned} E_6 : \quad P_\psi(x, y) &= x^3 + y^3 + 1 - \psi xy, \\ E_7 : \quad P_\psi(x, y) &= x^2 + y^4 + 1 - \psi xy, \\ E_8 : \quad P_\psi(x, y) &= x^2 + y^3 + 1 - \psi xy. \end{aligned} \quad (4.47)$$

The relation between the modulus parameters reads $1/z_0 = \psi^m$, so that the sigma model phase corresponds to the region $|\psi|^m > e^\beta$. Here we recall that $m = \{3, 4, 6\}$ and $e^\beta = \{27, 64, 432\}$ for the $E_{\{6,7,8\}}$ family respectively.

In the sigma model region $|\psi|^m > e^\beta$, the following expansion is valid:

$$\log(P_\psi) - \log(-xy\psi) = \log(1 - \psi^{-1}Q) = - \sum_{n=1}^{\infty} \frac{1}{n} \psi^{-n} Q^n, \quad (4.48)$$

where

$$\begin{aligned} E_6 : \quad Q(x, y) &= \frac{x^3 + y^3 + 1}{xy}, \\ E_7 : \quad Q(x, y) &= \frac{x^2 + y^4 + 1}{xy}, \\ E_8 : \quad Q(x, y) &= \frac{x^2 + y^3 + 1}{xy}. \end{aligned} \quad (4.49)$$

It can be seen that $\langle Q^n \rangle_0$ is zero unless $n = 0 \pmod m$; on the other hand

$$\begin{aligned} E_6 : \quad \langle Q^{3k} \rangle_0 &= \frac{\Gamma(3k+1)}{\Gamma(k+1)^3}, \\ E_7 : \quad \langle Q^{4k} \rangle_0 &= \frac{\Gamma(4k+1)}{\Gamma(k+1)^2 \Gamma(2k+1)}, \\ E_8 : \quad \langle Q^{6k} \rangle_0 &= \frac{\Gamma(6k+1)}{\Gamma(k+1) \Gamma(2k+1) \Gamma(3k+1)}. \end{aligned}$$

This can be succinctly expressed by $A(k)$ defined in (3.9) as

$$\langle Q^{mk} \rangle_0 = e^{k\beta} k A(k). \quad (4.50)$$

Using (4.45), (4.48) and (4.50), we obtain the relation between the constant term of $\log(P_\psi)$ and the large radius expansion of the period $U_1(z)$ (3.7)

$$\langle \log(P_\psi) \rangle_0 = \frac{1}{(2\pi i)^2} \int_{\mathbf{T}} \log(P_\psi) \frac{dx dy}{x y} = -\frac{1}{m} U_1 \left(\frac{e^\beta}{\psi^m} \right). \quad (4.51)$$

This is as expected because the middle term is nothing but the fundamental period of local mirror symmetry [14].

We see from (4.51) that in the sigma model region $|\psi|^m > e^\beta$, the Mahler measure of P_ψ (4.47) is essentially the same as the real Kähler modulus J of the corresponding local Calabi–Yau geometry:

$$E_6 : \quad \frac{3}{2\pi} m(P_\psi) = \operatorname{Im} \left\{ \frac{U_1}{2\pi i} \left(\frac{27}{\psi^3} \right) \right\} = J \left(\frac{27}{\psi^3} \right), \quad (4.52)$$

$$E_7 : \quad \frac{4}{2\pi} m(P_\psi) = \operatorname{Im} \left\{ \frac{U_1}{2\pi i} \left(\frac{64}{\psi^4} \right) \right\} = J \left(\frac{64}{\psi^4} \right), \quad (4.53)$$

$$E_8 : \quad \frac{6}{2\pi} m(P_\psi) = \operatorname{Im} \left\{ \frac{U_1}{2\pi i} \left(\frac{432}{\psi^6} \right) \right\} = J \left(\frac{432}{\psi^6} \right). \quad (4.54)$$

For the E_6 model, the Kähler modulus J in (4.52) can be represented as an Eisenstein–Kronecker–Lerch series [29], which gives the complete expression to (4.40)

$$\begin{aligned} J \left(\frac{27}{\psi^3} \right) &= \operatorname{Re} \left\{ \operatorname{Im} \tau + \frac{9}{2\pi} \sum_{n=1}^{\infty} \sum_{d|n} \chi(d) d^2 \frac{q^n}{n} \right\} \\ &= \frac{3^{\frac{9}{2}} \operatorname{Im} \tau}{(2\pi)^3} \operatorname{Re} \left\{ \sum'_{n,m \in \mathbf{Z}} \frac{\chi(n)}{(3m\tau + n)^2 (3m\bar{\tau} + n)} \right\}, \end{aligned} \quad (4.55)$$

where χ is the Dirichlet character defined in (3.63).

A quite remarkable relation between the Mahler measures and the special values of L -functions has been found [40, 30, 29]. Needless to say, a fully rigorous treatment of this subject is beyond our scope. Nevertheless we would like to quote here a conjecture from [29, p. 33], which has direct relevance to our problem: For $\psi \in \mathbf{Z}$, let $L(s, E_\psi)$ be the Hasse–Weil L -function of the corresponding elliptic curve E_ψ defined by (4.47). Then for

all sufficiently large ψ , the Mahler measure of P_ψ coincides with the special value of the L -function of E_ψ up to a multiplication by a nonzero rational number:

$$L'(0, E_\psi) = r_\psi m(P_\psi), \quad r_\psi \in \mathbf{Q}^*. \quad (4.56)$$

It follows immediately that the value of the real Kähler modulus $J(e^\beta/\psi^m)$ of the local Calabi–Yau geometry with ψ for which the conjecture (4.56) is valid can be given by the special value of the L -function of the elliptic curve E_ψ .

Take, for example, the E_8 model. Then the conjecture is rewritten as

$$J\left(\frac{432}{\psi^6}\right) = \frac{6}{2\pi} \frac{1}{r_\psi} L'(0, E_\psi), \quad r_\psi \in \mathbf{Q}^*. \quad (4.57)$$

In fact, the *numerical experiment* for the E_8 family of the curves by Boyd [30] shows the validity of the conjecture (4.56) for $3 \leq \psi \leq 18$.[¶] Borrowing his data, we list in Table 2 the values of the real Kähler modulus of our local Calabi–Yau model $J(\frac{432}{\psi^6})$ as well as the rational numbers r_ψ *unspecified* in the conjecture.

Now we consider the mirror map of the local Calabi–Yau model at the discriminant locus $z=1$. The value of the Kähler modulus at this point $J(1) = \text{Im}\{C_1/(2\pi i)\}$ is of great importance because it determines the asymptotic large k behavior of the Gromov–Witten invariant $n(k)$ according to (3.75). In this respect we would like to call $2\pi J(1) = -\text{Re } C_1$ the *entropy* of the local Calabi–Yau model. Note that at the discriminant locus the curve (4.47) is no longer elliptic by definition. Correspondingly, the L -function the special value of which yields that of the Kähler modulus J at $z=1$ becomes the Dirichlet one, which we repeat for convenience:

$$E_6 : J(1) = \frac{9}{2\pi} L'(-1, \chi_3) = 0.462757882001768178 \dots, \quad (4.58)$$

$$E_7 : J(1) = \frac{2}{2\pi} L'(-1, \chi_8) = 0.610262151883452845 \dots, \quad (4.59)$$

$$E_8 : J(1) = \frac{10}{2\pi} L'(-1, \chi_4) = 0.928067181776930407 \dots, \quad (4.60)$$

where (4.58) is proved in [29] while (4.59) and (4.60) are found by our numerical experiment. It must not be too difficult to prove the latter two equalities in a rigorous manner.

[¶]Note that $\psi=2$ is not in the sigma model phase, while the rapid growth of the conductor of the elliptic curve E_ψ makes it difficult to compute $L'(0, E_\psi)$ for $\psi > 18$.

ψ	r_ψ	$J(\frac{432}{\psi^6})$
3	-4/3	1.03304893002510628669 ...
4	-72	1.32141313308322098021 ...
5	168	1.53628426583345256681 ...
6	-216	1.71079907475933497399 ...
7	-1152	1.85812606670894012215 ...
8	2688	1.98568395763630817133 ...
9	1440	2.09817694280347199839 ...
10	10704	2.19879724623853723282 ...
11	-14400	2.28981592341485331429 ...
12	7920	2.37290786045027306396 ...
13	30888	2.44934423568787924171 ...
14	7488	2.52011284640251294912 ...
15	24480	2.58599661552298151995 ...
16	-155520	2.64762663264546979711 ...
17	-139392	2.70551905562125080466 ...
18	82368	2.76010143509263748236 ...

Table 2: Real Kähler modulus $J(\frac{432}{\psi^6})$ for E_8 del Pezzo model.

4.5 Monodromy matrices

Having fixed the mirror maps let us collect here all the monodromy matrices relevant to our consideration. For the orbifold models, if we take the basis $(1, t, t_d)$ the monodromy matrices, acting on ${}^t(1, t, t_d)$ from the left, with integral entries are obtained as in Table 3. Using the basis $(1, t_b, t_d)$, which will be adopted when discussing D-brane configurations on $\mathbf{P}(1, a, b)$, we have the result in Table 4. To be self-contained we also present in Table 5 the well-known monodromies for the $E_{6,7,8}$ tori acting on ${}^t(\varpi_0, -\varpi_1/(2\pi i))$. In particular, for E_6 and E_7 , the Picard–Fuchs monodromy generates $\Gamma_0(3)$ and $\Gamma_0(2)$, respectively. The monodromy matrices acting on ${}^t(1, t, t_{dP})$ in the dell Pezzo models are given in Table 6. We note again that the monodromy matrix M_∞ in Tables 3–6 obeys $(M_\infty)^m = I$ for the $\mathbf{Z}_{m=3,4,6}$ orbifolds and the $E_{6,7,8}$ tori as well as del Pezzo surfaces, and $M_\infty = M_1 M_0$.

	M_0	M_1	M_∞
\mathbf{Z}_3	$\begin{pmatrix} 1 & 0 & 0 \\ 1 & 1 & 0 \\ 0 & 1 & 1 \end{pmatrix}$	$\begin{pmatrix} 1 & 0 & 0 \\ 0 & 1 & -3 \\ 0 & 0 & 1 \end{pmatrix}$	$\begin{pmatrix} 1 & 0 & 0 \\ 1 & -2 & -3 \\ 0 & 1 & 1 \end{pmatrix}$
\mathbf{Z}_4	$\begin{pmatrix} 1 & 0 & 0 \\ 1 & 1 & 0 \\ 0 & 1 & 1 \end{pmatrix}$	$\begin{pmatrix} 1 & 0 & 0 \\ 0 & 1 & -2 \\ 0 & 0 & 1 \end{pmatrix}$	$\begin{pmatrix} 1 & 0 & 0 \\ 1 & -1 & -2 \\ 0 & 1 & 1 \end{pmatrix}$
\mathbf{Z}_6	$\begin{pmatrix} 1 & 0 & 0 \\ 1 & 1 & 0 \\ 0 & 1 & 1 \end{pmatrix}$	$\begin{pmatrix} 1 & 0 & 0 \\ 0 & 1 & -1 \\ 0 & 0 & 1 \end{pmatrix}$	$\begin{pmatrix} 1 & 0 & 0 \\ 1 & 0 & -1 \\ 0 & 1 & 1 \end{pmatrix}$

Table 3: The monodromy in the integral basis $(1, t, t_d)$ for the $\mathbf{Z}_{3,4,6}$ orbifold models.

	M_0	M_1	M_∞
\mathbf{Z}_3	$\begin{pmatrix} 1 & 0 & 0 \\ 1 & 1 & 0 \\ \frac{1}{2} & 1 & 1 \end{pmatrix}$	$\begin{pmatrix} 1 & 0 & 0 \\ 0 & 1 & -3 \\ 0 & 0 & 1 \end{pmatrix}$	$\begin{pmatrix} 1 & 0 & 0 \\ -\frac{1}{2} & -2 & -3 \\ \frac{1}{2} & 1 & 1 \end{pmatrix}$
\mathbf{Z}_4	$\begin{pmatrix} 1 & 0 & 0 \\ 1 & 1 & 0 \\ \frac{1}{2} & 1 & 1 \end{pmatrix}$	$\begin{pmatrix} 1 & 0 & 0 \\ 0 & 1 & -2 \\ 0 & 0 & 1 \end{pmatrix}$	$\begin{pmatrix} 1 & 0 & 0 \\ 0 & -1 & -2 \\ \frac{1}{2} & 1 & 1 \end{pmatrix}$
\mathbf{Z}_6	$\begin{pmatrix} 1 & 0 & 0 \\ 1 & 1 & 0 \\ \frac{1}{2} & 1 & 1 \end{pmatrix}$	$\begin{pmatrix} 1 & 0 & 0 \\ 0 & 1 & -1 \\ 0 & 0 & 1 \end{pmatrix}$	$\begin{pmatrix} 1 & 0 & 0 \\ \frac{1}{2} & 0 & -1 \\ \frac{1}{2} & 1 & 1 \end{pmatrix}$

Table 4: The monodromy in the basis $(1, t_b, t_d)$ for the $\mathbf{Z}_{3,4,6}$ orbifold models.

	M_0	M_1	M_∞
E_6	$\begin{pmatrix} 1 & 0 \\ 1 & 1 \end{pmatrix}$	$\begin{pmatrix} 1 & -3 \\ 0 & 1 \end{pmatrix}$	$\begin{pmatrix} -2 & -3 \\ 1 & 1 \end{pmatrix}$
E_7	$\begin{pmatrix} 1 & 0 \\ 1 & 1 \end{pmatrix}$	$\begin{pmatrix} 1 & -2 \\ 0 & 1 \end{pmatrix}$	$\begin{pmatrix} -1 & -2 \\ 1 & 1 \end{pmatrix}$
E_8	$\begin{pmatrix} 1 & 0 \\ 1 & 1 \end{pmatrix}$	$\begin{pmatrix} 1 & -1 \\ 0 & 1 \end{pmatrix}$	$\begin{pmatrix} 0 & -1 \\ 1 & 1 \end{pmatrix}$

Table 5: The monodromy for the $E_{6,7,8}$ tori.

	M_0	M_1	M_∞
E_6	$\begin{pmatrix} 1 & 0 & 0 \\ 1 & 1 & 0 \\ 0 & 1 & 1 \end{pmatrix}$	$\begin{pmatrix} 1 & 0 & 0 \\ -1 & 1 & -3 \\ 0 & 0 & 1 \end{pmatrix}$	$\begin{pmatrix} 1 & 0 & 0 \\ 0 & -2 & -3 \\ 0 & 1 & 1 \end{pmatrix}$
E_7	$\begin{pmatrix} 1 & 0 & 0 \\ 1 & 1 & 0 \\ 0 & 1 & 1 \end{pmatrix}$	$\begin{pmatrix} 1 & 0 & 0 \\ -1 & 1 & -2 \\ 0 & 0 & 1 \end{pmatrix}$	$\begin{pmatrix} 1 & 0 & 0 \\ 0 & -1 & -2 \\ 0 & 1 & 1 \end{pmatrix}$
E_8	$\begin{pmatrix} 1 & 0 & 0 \\ 1 & 1 & 0 \\ 0 & 1 & 1 \end{pmatrix}$	$\begin{pmatrix} 1 & 0 & 0 \\ -1 & 1 & -1 \\ 0 & 0 & 1 \end{pmatrix}$	$\begin{pmatrix} 1 & 0 & 0 \\ 0 & 0 & -1 \\ 0 & 1 & 1 \end{pmatrix}$

Table 6: The monodromy in the basis $(1, t, t_{dP})$ for the $E_{6,7,8}$ del Pezzo models.

5 D-branes wrapping a surface

In the previous section we have determined how a complexified Kähler class of a surface S embedded in a non-compact Calabi–Yau threefold X depends on a modulus parameter z in the orbifold models for which $S = \mathbf{P}(1, a, b)$ with $(a, b) = (1, 1), (1, 2), (2, 3)$, and in the local del Pezzo models for which $S = E_{6,7,8}$ del Pezzo surfaces. The result is now employed to discuss D-brane configurations on S . The RR charge vector of D-branes wrapped on S is given by [41, 42]

$$Q = \text{ch}(V) \sqrt{\frac{\text{Todd}(T_S)}{\text{Todd}(N_S)}} \in \bigoplus_{i=0}^2 H^{2i}(S, \mathbf{Q}), \quad (5.1)$$

where V is a vector bundle on S (or, more precisely, a coherent \mathcal{O}_S -module), $\text{ch}(V)$ is the Chern character; $\text{ch}(V) = r(V) + c_1(V) + \text{ch}_2(V)$ and T_S (N_S) is the tangent (normal) bundle to S . The BPS central charge then takes the form in the large radius region

$$Z = - \int_S e^{-J_S} \text{ch}(V) \sqrt{\frac{\text{Todd}(T_S)}{\text{Todd}(N_S)}} + \dots, \quad (5.2)$$

where J_S is a Kähler class of S compatible with an embedding $S \hookrightarrow X$ and the ellipses stand for possible world-sheet instanton corrections. Notice that in the present embedding, N_S is isomorphic to the canonical line bundle K_S , and hence $c_1(N_S) = -c_1(S)$.

5.1 Local del Pezzo models

The configuration of D-branes on a del Pezzo surface embedded in a Calabi–Yau threefold X has been studied in [43, 44, 24]. Let us begin with presenting some computations based on a description of $E_{6,7,8}$ del Pezzo surfaces as hypersurfaces in weighted projective space. Let S denote $E_{6,7,8}$ del Pezzo surfaces. As explained in section 2.4, S is realized as a hypersurface of degree $(1 + a + b)$ in $\mathbf{P}(1, 1, a, b)$ where $(a, b) = (1, 1), (1, 2), (2, 3)$ for $E_{6,7,8}$ respectively. Let D be a divisor of $\mathbf{P}(1, 1, a, b)$ isomorphic to $\mathbf{P}(1, a, b)$ and denote $\bar{D} = D \cap S$. \bar{D} has the self-intersection

$$\bar{D} \cdot \bar{D} = \frac{1 + a + b}{ab} = 9 - N \quad (5.3)$$

for $E_{N=6,7,8}$. Calculating the total Chern class with the use of the adjunction formula one obtains $c_1(S) = \bar{D}$, and $c_2(S) = (a + b + ab)\bar{D} \cdot \bar{D}$ from which the Euler characteristic of S , that is, $\chi(S) = 3 + N$, can be reproduced. The calculation of the Todd class yields

$$\sqrt{\frac{\text{Todd}(T_S)}{\text{Todd}(N_S)}} = 1 + \frac{1}{2}\bar{D} + \frac{15 - N}{12}w_S, \quad (5.4)$$

where $w_S = \frac{1}{9-N}\bar{D}^2$ and $c_1(N_S) = -\bar{D}$, which holds in the present embedding $S \hookrightarrow X$, has been utilized.

Since the first Chern class of S is ample, we take the Kähler class $J_S = t\bar{D}$ and write down the central charge in the large radius limit [24]

$$\begin{aligned} Z &= - \int_S e^{-t\bar{D}} \text{ch}(V) \sqrt{\frac{\text{Todd}(T_S)}{\text{Todd}(N_S)}} + \mathcal{O}(e^{2\pi it}) \\ &= -r\bar{D} \cdot \bar{D} \left(\frac{t^2}{2} - \frac{t}{2} + \frac{1}{12} \frac{3 - N}{9 - N} \right) + d(V)t - \chi(V) + \mathcal{O}(e^{2\pi it}), \end{aligned} \quad (5.5)$$

where $d(V) = c_1(V) \cdot \bar{D}$ and the Euler characteristic of V is given by $\chi(V) = r(V) + \frac{1}{2}d(V) + k(V)$ with $k(V) = \int_S \text{ch}_2(V)$.

At a generic point of the moduli space, the central charge for the local del Pezzo models reads

$$Z = n_4 \bar{D} \cdot \bar{D} t_{dP} + n_2 t + n_0, \quad (5.6)$$

where n_i are integers. The model is dual to a theory on a D3-brane probing the affine 7-brane backgrounds, in view of which n_i are string junction charges [24]. In the large radius limit it is clear from (4.13) that (5.6) reduces to (5.5). Thus, if a BPS state with the charge vector (n_0, n_2, n_4) survives all the way down to the large radius limit at $z = 0$ it should admit a description in terms of coherent sheaves on S under the relation [43, 24]

$$n_0 = -\chi(V), \quad n_2 = d(V), \quad n_4 = -r(V). \quad (5.7)$$

It also follows that $\bar{D} \cdot \bar{D} t_{dP}$ gives a normalized central charge of a D4-brane. A bundle (or sheaf in general) V corresponds to a D-brane with the positive orientation if $r(V) > 0$, or $r(V) = 0$ and $d(V) > 0$, or $r(V) = d(V) = 0$ and $\chi(V) < 0$, and otherwise to a D-brane with the opposite orientation, which we call a \bar{D} -brane.

The homology $H_2(S, \mathbf{Z})$ of an E_N del Pezzo surface is spanned by a generic line ℓ in \mathbf{P}^2 and the exceptional divisors e_1, \dots, e_N of the blown-up points. The degree zero sublattice of $H_2(S)$ is isomorphic to the E_N root lattice with the simple roots; $\alpha_i = e_i - e_{i+1}$ ($1 \leq i \leq N-1$) and $\alpha_N = \ell - e_1 - e_2 - e_3$. Then the first Chern class $c_1(V)$ has the orthogonal decomposition [24]

$$c_1(V) = \frac{d(V)}{9-N} \bar{D} + \sum_{i=1}^N \lambda_i(V) \mathbf{w}^i, \quad (5.8)$$

where $\mathbf{w}^i \cdot \alpha_j = -\delta_j^i$ and $\bar{D} \cdot \mathbf{w}^i = 0$. Thus the D2-brane charge is specified not only by the degree $d(V)$ but also by the Dynkin label $\{\lambda_i\}$ of a representation of E_N . If we turn on all the Kähler parameters associated with the exceptional divisors, the central charge formula (5.6) will be modified so as to contain the full dependence on $\{\lambda_i\}$. The second Chern class $c_2(V)$ is now evaluated from (5.7) and (5.8) to be

$$\int_S c_2(V) = n_0 + \frac{n_2}{2} + \frac{1}{2} \left(\frac{n_2^2}{9-N} - \lambda \cdot \lambda \right) - n_4. \quad (5.9)$$

Eqs. (5.7) and (5.9) enable us to translate the charge vector (n_0, n_2, n_4) into the sheaf data (modulo the E_N representation).

At $z = \infty$, the $E_{N=6,7,8}$ del Pezzo model exhibits a $\mathbf{Z}_{3,4,6}$ symmetry, respectively. Since $t = t_{dP} = 0$ at $z = \infty$, a BPS state with $n_0 = 0$ becomes massless, but a state with $n_0 \neq 0$ massive. Let us present typical examples of $\mathbf{Z}_{3,4,6}$ orbits of BPS states. In view

of a D3-probe theory [24], we observe that a state with $(n_0, n_2, n_4) = (1, 0, 1)$ is BPS, E_N singlet and exists everywhere in the moduli space. In fact, according to (5.7), this state is identified with a $\overline{\text{D4}}$ -brane corresponding to $-\mathcal{O}$ with \mathcal{O} being the trivial line bundle. At $z = \infty$, the state $(1, 0, 1)$ remains massive and its \mathbf{Z}_m orbits are constructed by the $\mathbf{Z}_{3,4,6}$ action on the charge vector

$$(n_0, n_2, n_4) \rightarrow (n_0, n_2, n_4) \begin{pmatrix} 1 & 0 & 0 \\ 0 & N-8 & -1 \\ 0 & 9-N & 1 \end{pmatrix}. \quad (5.10)$$

This has been obtained from Table 6 by noting that the monodromy matrices acting on the periods ${}^t(1, t, t_{dP})$ by left multiplication act on the charge vector (n_0, n_2, n_4) by right multiplication. We then have the E_N singlet massive \mathbf{Z}_m orbits associated with the state $(1, 0, 1)$ and corresponding D-brane configurations as follows:

- E_6 del Pezzo

$$\begin{aligned} (1, 0, 1) &\rightarrow \overline{\text{D4}}, \\ (1, 3, 1) &\rightarrow \overline{\text{D4}} + \text{D2}, \\ (1, -3, -2) &\rightarrow 2\text{D4} + \overline{\text{D2}} + 3\text{D0}. \end{aligned} \quad (5.11)$$

- E_7 del Pezzo

$$\begin{aligned} (1, 0, 1) &\rightarrow \overline{\text{D4}}, \\ (1, 2, 1) &\rightarrow \overline{\text{D4}} + \text{D2}, \\ (1, 0, -1) &\rightarrow \text{D4} + 2\text{D0} \\ (1, -2, -1) &\rightarrow \text{D4} + \overline{\text{D2}} + 2\text{D0}. \end{aligned} \quad (5.12)$$

- E_8 del Pezzo

$$\begin{aligned} (1, 0, 1) &\rightarrow \overline{\text{D4}}, \\ (1, 1, 1) &\rightarrow \overline{\text{D4}} + \text{D2}, \\ (1, 1, 0) &\rightarrow \text{D2} + 2\text{D0}, \\ (1, 0, -1) &\rightarrow \text{D4} + 2\text{D0}, \\ (1, -1, -1) &\rightarrow \text{D4} + \overline{\text{D2}} + 2\text{D0}, \\ (1, -1, 0) &\rightarrow \overline{\text{D2}}. \end{aligned} \quad (5.13)$$

Note that every D2 (or $\overline{\text{D2}}$)-brane in the above is E_N singlet. It will be very interesting to have a proper interpretation of these configurations in terms of vector bundles on del Pezzo surfaces.

Finally let us remark how the monodromy action on the periods induces the corresponding action on a vector bundle. As just mentioned above, we know how the monodromy acts on the charge vector, and hence we can convert the large radius monodromy action on the periods to that on the vector bundle under the identification (5.7). The result is

$$\text{ch}(V) \rightarrow \text{ch}(V) e^{-\bar{D}}, \quad (5.14)$$

which is in accordance with the fact that the large radius monodromy $t \rightarrow t+1$ is induced by a shift of the B-field; $B \rightarrow B+1$. Similarly the monodromy at $z=1$ leads to

$$\text{ch}(V) \rightarrow \text{ch}(V) + \int_S \text{ch}(V) \bar{D}. \quad (5.15)$$

This is understood to be performed along a loop which is based at the point $z=0$ (the large radius limit) and encircles the discriminant locus at $z=1$ [45, 46]. See [4] for a related observation in the case of an elliptically fibered Calabi–Yau model.

5.2 Orbifold models

Let us next turn to the orbifold models. As we have described in section 2.1, the blown-up orbifold $\text{Bl}_{\nu_0}(\mathbf{C}^3/\mathbf{Z}_m)$ has an exceptional divisor $\mathbf{P}(1, a, b)$ with $(a, b) = (1, 1), (1, 2), (2, 3)$, respectively. In this section we consider D-branes wrapped on $S = \mathbf{P}(1, a, b)$. When applying (5.1) to the computation of D-brane charges one should take into account that the background B-field is turned on in the orbifold model as shown in (4.5). Following [3, 10] we assume that the B -dependence of $\text{ch}(V)$ will cancel out the factor $e^{c_1(S)/2}$ appearing in the relation

$$\sqrt{\frac{\text{Todd}(T_S)}{\text{Todd}(K_S)}} = e^{\frac{1}{2}c_1(S)} \sqrt{\frac{\widehat{A}(T_S)}{\widehat{A}(K_S)}} \quad (5.16)$$

so that the RR charge vector is read off from

$$Q = \text{ch}(V) \sqrt{\frac{\widehat{A}(T_S)}{\widehat{A}(K_S)}}. \quad (5.17)$$

Let us set the Kähler class $J_S = t_b D$, where D is the ample generator of divisors of S , then the classical central charge (5.2) takes the form

$$Z = - \int_S e^{-t_b D} \text{ch}(V) \sqrt{\frac{\widehat{A}(T_S)}{\widehat{A}(K_S)}} + \text{O}(e^{2\pi i t_b}). \quad (5.18)$$

The quantum central charge, on the other hand, is expressed in terms of the periods as

$$Z(n_0, n_2, n_4) = n_4 D \cdot D t_d + n_2 t_b + n_0, \quad (5.19)$$

where n_i are not necessarily integral. We now wish to show that, in the large radius limit, (5.18) is precisely recovered from (5.19). For this we first give the self-intersection of D

$$D \cdot D = \frac{1}{ab} = 1, \quad \frac{1}{2}, \quad \frac{1}{6} \quad (5.20)$$

for $\mathbf{C}^3/\mathbf{Z}_{3,4,6}$. Next, using the naive adjunction formula we obtain

$$\sqrt{\frac{\widehat{A}(T_S)}{\widehat{A}(K_S)}} = 1 + \frac{1}{24} \tilde{\chi}(S) w_S, \quad (5.21)$$

where $\tilde{\chi}(S) = (a+b+ab)/(ab)$ and $w_S = abD^2$. The classical central charge (5.18) thereby turns out to be

$$\begin{aligned} Z &= -\frac{1}{2} r(V) D \cdot D t_b^2 + d(V) t_b - \frac{1}{24} r(V) \tilde{\chi}(S) - k(V) + \text{O}(e^{2\pi i t_b}) \\ &= -r(V) D \cdot D \left(\frac{t_b^2}{2} + \frac{a+b+ab}{24} \right) + d(V) t_b - k(V) + \text{O}(e^{2\pi i t_b}), \end{aligned} \quad (5.22)$$

where $d(V) = c_1(V) \cdot D$ and $k(V) = \int_S \text{ch}_2(V)$. It is clearly seen that if we put

$$n_0 = -k(V), \quad n_2 = d(V), \quad n_4 = -r(V), \quad (5.23)$$

(5.22) coincides with (5.19) by virtue of (4.12) in the large radius region.

In (5.19), thus, $D \cdot D t_d$ plays a role of the normalized central charge of a D4-brane. Since we have $c_1(V) = ab d(V) D$, the second Chern class is obtained as

$$\int_S c_2(V) = n_0 + \frac{1}{2} ab n_2^2. \quad (5.24)$$

Using (5.23) and (5.24) one can convert the orbifold charges (n_0, n_2, n_4) into the sheaf data in the large radius region. When doing this, the data with negative $r(V)$ as well as $r(V) = 0$ is treated as in the case of local del Pezzo models.

Let us concentrate on the orbifold point $z = \infty$. Since $t_d(z = \infty) = \frac{1}{\lambda}(= \frac{1}{3}, \frac{1}{2}, 1)$ we have a particular value of the central charge

$$Z(0, 0, 1) = D \cdot D \frac{1}{\lambda} = \frac{1}{ab\lambda} = \frac{1}{m} \quad (5.25)$$

for the $\mathbf{C}^3/\mathbf{Z}_{m=3,4,6}$ models. This is regarded as $1/m$ of the mass of a D0-brane. Therefore the configuration $(0, 0, 1)$ is identified with a fractional brane. At the orbifold point there exists a \mathbf{Z}_m quantum symmetry. Following the del Pezzo case one can read off from Table 4 the \mathbf{Z}_m action on the charge vector

$$(n_0, n_2, n_4) \rightarrow (n_0, n_2, n_4) \begin{pmatrix} 1 & 0 & 0 \\ 1 - \frac{\lambda}{2} & 1 - \lambda & -m \\ \frac{\lambda}{2m} & \frac{\lambda}{m} & 1 \end{pmatrix}. \quad (5.26)$$

Thus the \mathbf{Z}_3 orbit of fractional branes in the \mathbf{Z}_3 orbifold model reads

$$(0, 0, 1) \rightarrow \left(\frac{1}{2}, 1, 1\right) \rightarrow \left(\frac{1}{2}, -1, -2\right). \quad (5.27)$$

For the \mathbf{Z}_4 orbifold we have the \mathbf{Z}_4 orbit

$$(0, 0, 1) \rightarrow \left(\frac{1}{4}, \frac{1}{2}, 1\right) \rightarrow \left(\frac{1}{2}, 0, -1\right) \rightarrow \left(\frac{1}{4}, -\frac{1}{2}, -1\right). \quad (5.28)$$

Likewise the \mathbf{Z}_6 orbifold model has the \mathbf{Z}_6 orbit of fractional branes

$$(0, 0, 1) \rightarrow \left(\frac{1}{12}, \frac{1}{6}, 1\right) \rightarrow \left(\frac{1}{4}, \frac{1}{6}, 0\right) \rightarrow \left(\frac{1}{3}, 0, -1\right) \rightarrow \left(\frac{1}{4}, -\frac{1}{6}, -1\right) \rightarrow \left(\frac{1}{12}, -\frac{1}{6}, 0\right). \quad (5.29)$$

These fractional branes are constructed as the boundary states of the $\mathbf{C}^3/\mathbf{Z}_m$ orbifold CFT at $z = \infty$ [3]. If we assume that these BPS states are stable in the large radius limit, they should be described as coherent sheaves on S . The states in the \mathbf{Z}_m orbit are then identified with the corresponding D-brane configurations by the use of (5.23), (5.24). Corresponding to the \mathbf{Z}_m orbits, we get the following D-brane configurations:

- \mathbf{Z}_3 orbifold

$$\begin{aligned} (0, 0, 1) &\rightarrow \overline{\text{D4}}, \\ \left(\frac{1}{2}, 1, 1\right) &\rightarrow \overline{\text{D4}} + \text{D2}, \\ \left(\frac{1}{2}, -1, -2\right) &\rightarrow 2\text{D4} + \overline{\text{D2}} + \text{D0}. \end{aligned} \quad (5.30)$$

Here the first two configurations are identified with $-\mathcal{O}$, $-\mathcal{O}(-1)$, where \mathcal{O} , $\mathcal{O}(-1)$ are the trivial and the tautological line bundles on \mathbf{P}^2 , whereas the third one is a rank two exceptional bundle on \mathbf{P}^2 [3]. We will review exceptional bundles on \mathbf{P}^2 in Appendix A.

- \mathbf{Z}_4 orbifold

$$\begin{aligned}
(0, 0, 1) &\rightarrow \overline{\mathbf{D}4}, \\
\left(\frac{1}{4}, \frac{1}{2}, 1\right) &\rightarrow \overline{\mathbf{D}4} + \mathbf{D}2, \\
\left(\frac{1}{2}, 0, -1\right) &\rightarrow \mathbf{D}4 + \frac{1}{2}\mathbf{D}0, \\
\left(\frac{1}{4}, -\frac{1}{2}, -1\right) &\rightarrow \mathbf{D}4 + \overline{\mathbf{D}2} + \frac{1}{2}\mathbf{D}0.
\end{aligned} \tag{5.31}$$

- \mathbf{Z}_6 orbifold

$$\begin{aligned}
(0, 0, 1) &\rightarrow \overline{\mathbf{D}4}, \\
\left(\frac{1}{12}, \frac{1}{6}, 1\right) &\rightarrow \overline{\mathbf{D}4} + \mathbf{D}2, \\
\left(\frac{1}{4}, \frac{1}{6}, 0\right) &\rightarrow \mathbf{D}2 + \frac{1}{3}\mathbf{D}0, \\
\left(\frac{1}{3}, 0, -1\right) &\rightarrow \mathbf{D}4 + \frac{1}{3}\mathbf{D}0, \\
\left(\frac{1}{4}, -\frac{1}{6}, -1\right) &\rightarrow \mathbf{D}4 + \overline{\mathbf{D}2} + \frac{1}{3}\mathbf{D}0, \\
\left(\frac{1}{12}, -\frac{1}{6}, 0\right) &\rightarrow \overline{\mathbf{D}2}.
\end{aligned} \tag{5.32}$$

In the \mathbf{Z}_4 and \mathbf{Z}_6 cases, D-branes wrap $\mathbf{P}(1, 1, 2)$ and $\mathbf{P}(1, 2, 3)$ respectively. Remember that $\mathbf{P}(1, 1, 2) \simeq \mathbf{P}^2/\mathbf{Z}_2$ and $\mathbf{P}(1, 2, 3) \simeq \mathbf{P}^2/\mathbf{Z}_2 \times \mathbf{Z}_3$. Namely D-branes are on orbifolds with quotient singularities yet to be resolved. This may result in the fractional values of the second Chern class we have observed in the above \mathbf{Z}_4 and \mathbf{Z}_6 orbits.

Finally we note that the large radius monodromy acts on the Chern character as

$$\text{ch}(V) \rightarrow \text{ch}(V) e^{-D}, \tag{5.33}$$

while under the monodromy at $z = 1$ one has

$$\text{ch}(V) \rightarrow \text{ch}(V) + m \int_S \text{ch}(V) D, \tag{5.34}$$

where $mD = c_1(S)$ is the first Chern class of $\mathbf{P}(1, a, b)$ with $m = 1 + a + b$.

5.3 Monodromy invariant intersection form

Let $\iota: S \hookrightarrow X$ be an embedding of a surface S in a Calabi–Yau threefold X . We then have the direct image map ι_* from the coherent \mathcal{O}_S -modules to the coherent \mathcal{O}_X -modules. The canonical intersection form on the vector bundles on X is given by

$$\begin{aligned} I_X(W_1, W_2) &= \int_X \text{ch}(W_1^*) \text{ch}(W_2) \text{Todd}(T_X), \\ &= -I_X(W_2, W_1), \end{aligned} \tag{5.35}$$

which can be extended to an anti-symmetric intersection form on the coherent \mathcal{O}_X -modules using locally-free resolutions of them.

The intersection form on the vector bundles on S induced from that on the ambient Calabi–Yau threefold X by the embedding $\iota: S \hookrightarrow X$ reads [24]

$$A_S(V_1, V_2) := I_X(\iota_* V_1, \iota_* V_2) = r(V_1) d(V_2) - r(V_2) d(V_1), \tag{5.36}$$

where $d(V) = c_1(V) \cdot c_1(S)$ is the degree of the bundle. Note that for $S = \mathbf{P}(1, a, b)$, $d(V)$ here is m times larger than that in the preceding subsection.

A_S does not depend on the detail of the embedding data, but only on the intrinsic geometry of S . More importantly, it is easily verified that A_S defines a *monodromy invariant* intersection form on the D-branes both on the $E_{6,7,8}$ del Pezzo surfaces and on the exceptional divisors $\mathbf{P}(1, a, b)$ of the $\mathbf{Z}_{3,4,6}$ orbifolds.

Acknowledgements

S.K.Y. would like to thank the participants of Summer Institute 2000 at Yamanashi, Japan, for their interest in the present work, especially T. Eguchi, K. Hori, H. Kanno, A. Kato and T. Kawai for stimulating discussions. We would like to thank Y. Ohtake for useful discussions. The research of K.M. and S.K.Y. was supported in part by Grant-in-Aid for Scientific Research on Priority Area 707 “Supersymmetry and Unified Theory of Elementary Particles”, Japan Ministry of Education, Science and Culture.

Appendix A Exceptional bundles on \mathbf{P}^2

The intersection pairing $\chi_{\mathbf{P}^2}$ on vector bundles on \mathbf{P}^2 is defined by

$$\begin{aligned}\chi_{\mathbf{P}^2}(V_1, V_2) &= \sum_{i=0}^2 (-1)^i \dim H^i(\mathbf{P}^2, \text{Hom}(V_1, V_2)), \\ &= r_1 r_2 + r_1 k_2 + r_2 k_1 - d_1 d_2 + \frac{3}{2}(r_1 d_2 - r_2 d_1),\end{aligned}\tag{A.1}$$

where $\text{Hom}(V_1, V_2) \cong V_1^* \otimes V_2$ is the homomorphism bundle, and we have used the Riemann–Roch formula [24] with the abbreviated notation: $r_{1,2} = r(V_{1,2})$, $d_{1,2} = d(V_{1,2})$, $k_{1,2} = k(V_{1,2})$ understood. In particular, the self-intersection of the bundle V becomes

$$\chi_{\mathbf{P}^2}(V, V) = \sum_{i=0}^2 (-1)^i \dim H^i(\mathbf{P}^2, \text{End}(V)) = r^2 + 2rk - d^2.\tag{A.2}$$

It must not be confused with the Euler characteristic of V defined by

$$\chi(V) = \sum_{i=0}^2 (-1)^i \dim H^i(\mathbf{P}^2, V) = r + \frac{3}{2}d + k.\tag{A.3}$$

We also introduce two other invariants of V , that is, the slope $\mu(V)$ and the (normalized) discriminant $\Delta(V)$, which must be positive for V to be stable:

$$\mu(V) = \frac{d}{r},\tag{A.4}$$

$$\Delta(V) = \frac{1}{2} \left(\frac{d}{r} \right)^2 - \frac{k}{r},\tag{A.5}$$

as well as the polynomial $P(z) = 1/2(z+1)(z+2)$ for convenience. We can then easily verify the following

$$\begin{aligned}\chi(V) &= r(P(\mu) - \Delta), \\ \chi(V_1, V_2) &= r_1 r_2 (P(\mu_2 - \mu_1) - \Delta_1 - \Delta_2).\end{aligned}\tag{A.6}$$

A vector bundle E on \mathbf{P}^2 is called *exceptional* if

$$H^0(\mathbf{P}^2, \text{End}(E)) \cong \mathbf{C}, \quad H^1(\mathbf{P}^2, \text{End}(E)) = 0, \quad H^2(\mathbf{P}^2, \text{End}(E)) = 0.$$

It is known that each exceptional bundle is stable, that is, its slope is greater than that of any coherent subsheaf of it, and has no moduli, which means that the complex structure

of an exceptional bundle is uniquely determined by its topological invariant (r, d, k) . In fact if E is exceptional, then k is not an independent degree of freedom but is written as $k = (1 + d^2 - r^2)/(2r)$ because

$$\chi_{\mathbf{P}^2}(E, E) = 1 \tag{A.7}$$

by definition. The remaining two $(r(E), d(E))$ must be *mutually prime* according to the formula (A.2). Therefore we have seen that *an exceptional bundle E is uniquely determined by its slope $\mu(E) = d/r$* . It is also easy to see that if E is exceptional then its discriminant reads

$$0 < \Delta(E) = \frac{1}{2} \left(1 - \frac{1}{r^2} \right) < \frac{1}{2}. \tag{A.8}$$

The exceptional bundles on \mathbf{P}^2 are completely classified in [47]. Because both the Peccei–Quinn symmetry $B \rightarrow B+1$ discussed in the preceding subsection, which operates as $E \rightarrow E(-1)$ so that $\mu \rightarrow \mu-1$, and the duality transformation $E \rightarrow E^*$, which results in $\mu \rightarrow -\mu$, preserve the endmorphism bundle $End(E)$, it suffices to list the rational numbers corresponding to the slopes of the exceptional bundles in the fundamental domain $[0, 1/2]$.

In order to state the result in [47], we must first introduce some notations closely following them. For $\alpha \in \mathbf{Q}$, the rank of it, which we denote by r_α , is the least positive number such that $\alpha r_\alpha \in \mathbf{Z}$. We also define its discriminant and Euler number by

$$\Delta_\alpha = \frac{1}{2} \left(1 - \frac{1}{r_\alpha^2} \right), \quad \chi_\alpha = r_\alpha (P(\alpha) - \Delta_\alpha).$$

For $\alpha, \beta \in \mathbf{Q}$, such that $\beta - \alpha - 3 \neq 0$, we define a third element of \mathbf{Q} by

$$\alpha \circ \beta := \frac{1}{2}(\alpha + \beta) + \frac{\Delta_\beta - \Delta_\alpha}{3 + \alpha - \beta}.$$

Let \mathcal{D} be the subset of \mathbf{Q} defined by

$$\mathcal{D} = \left\{ \frac{n}{2^q} \mid n \in \mathbf{Z}, q \in \mathbf{N} \cup \{0\} \right\}.$$

We can define the map $\varepsilon: \mathcal{D} \rightarrow \mathbf{Q}$ uniquely by the requirements: $\varepsilon(n) = n$ for $n \in \mathbf{Z}$, and

$$\varepsilon \left(\frac{2m+1}{2^{q+1}} \right) = \varepsilon \left(\frac{m}{2^q} \right) \circ \varepsilon \left(\frac{m+1}{2^q} \right).$$

It follows immediately that ε is strictly increasing function, $\varepsilon(\alpha+n) = \varepsilon(\alpha)+n$ for $n \in \mathbf{Z}$, $\varepsilon(-\alpha) = -\varepsilon(\alpha)$, and if $\alpha \in \mathcal{D}$, then $r_{\varepsilon(\alpha)} \geq r_\alpha$.

The fundamental result of [47] is that the set of exceptional bundles on \mathbf{P}^2 is identified by their slopes with the subset $\text{Im}(\varepsilon) = \text{Im}(\varepsilon: \mathcal{D} \rightarrow \mathbf{Q})$ of \mathbf{Q} . Note that from the property of the map ε , the slope μ of each exceptional bundle on \mathbf{P}^2 with $r < 2^{q+1}$ can be put in the finite set

$$\left\{ \varepsilon\left(\frac{m}{2^q}\right) \mid 1 \leq m \leq 2^{q-1} \right\} \subset \mathbf{Q} \cap \left[0, \frac{1}{2}\right], \quad (\text{A.9})$$

if we use the symmetries $\mu \rightarrow \mu - 1$ and $\mu \rightarrow -\mu$ discussed above.

Searching for the elements of $\text{Im}(\varepsilon) \cap [0, 1/2]$ with $2 \leq r < 64$, for example, we find, in addition to $(r, d, k) = (2, 1, -1/2)$, which is the dual of the rank two bundle appeared in the \mathbf{Z}_3 -orbit of the fractional branes (5.30), the four higher rank exceptional bundles [48]:

$$(r, d, k) = (5, 2, -2), \left(13, 5, -\frac{11}{2}\right), (29, 12, -12), \left(34, 13, -\frac{29}{2}\right). \quad (\text{A.10})$$

References

- [1] See, for a recent review, M.R. Douglas, Topics in D-geometry, *Class. Quant. Grav.* **17** (2000) 1057–1070, hep-th/9910170.
- [2] I. Brunner, M.R. Douglas, A. Lawrence and C. Römelsberger, D-Branes on the Quintic, *JHEP* **0008** (2000) 015, hep-th/9906200.
- [3] D.-E. Diaconescu and J. Gomis, Fractional Branes and Boundary States in Orbifold Theories, hep-th/9906242.
- [4] D.-E. Diaconescu and C. Römelsberger, D-Branes and Bundles on Elliptic Fibrations, *Nucl. Phys.* **B574** (2000) 245–262, hep-th/9910172.
- [5] P. Kaste, W. Lerche, C.A. Lütken and J. Walcher, D-Branes on K3-Fibrations, *Nucl. Phys.* **B582** (2000) 203–215, hep-th/9912147.
- [6] E. Scheidegger, D-Branes on Some One- and Two-Parameter Calabi–Yau Hypersurfaces, *JHEP* **0004** (2000) 003, hep-th/9912188.
- [7] B.R. Greene and C.I. Lazaroiu, Collapsing D-Branes in Calabi–Yau Moduli Space: I, hep-th/0001025
- [8] C.I. Lazaroiu, Collapsing D-Branes in One-Parameter Models and Small/Large Radius Duality, hep-th/0002004.
- [9] M.R. Douglas, B. Fiol and C. Römelsberger, Stability and BPS Branes, hep-th/0002037.
- [10] M.R. Douglas, B. Fiol and C. Römelsberger, The Spectrum of BPS Branes on a Noncompact Calabi–Yau, hep-th/0003263.
- [11] F. Denef, Supergravity Flows and D-Brane Stability, hep-th/0005049.
- [12] B. Fiol and M. Mariño, BPS States and Algebras from Quivers, *JHEP* **0007** (2000) 031, hep-th/0006189.

- [13] D.-E. Diaconescu and M.R. Douglas, D-Branes on Stringy Calabi–Yau Manifolds, hep-th/0006224.
- [14] T.-M. Chiang, A. Klemm, S.-T. Yau and E. Zaslow, Local Mirror Symmetry: Calculations and Interpretations, *Adv. Theor. Math. Phys.* **3** (1999), hep-th/9903053.
- [15] T. Oda, *Convex Bodies and Algebraic Geometry: An Introduction to the Theory of Toric Varieties*, *Ergebnisse der Mathematik und ihrer Grenzgebiete, 3 Folge Band 15*, Springer-Verlag, Berlin (1988).
- [16] W. Fulton, *Introduction to Toric Varieties*, *Annals of Mathematics Studies 131*, Princeton Univ. Press, Princeton (1993).
- [17] V.V. Batyrev, Variations of the Mixed Hodge Structure of Affine Hypersurfaces in Algebraic Tori, *Duke Math. J.* **69** (1993) 349–409.
- [18] S. Hosono, A. Klemm, S. Theisen and S.-T. Yau, Mirror Symmetry, Mirror Map and Applications to Calabi–Yau Hypersurfaces, *Commun. Math. Phys.* **167** (1995) 301–350, hep-th/9308122; Mirror Symmetry, Mirror Maps and Applications to Complete Intersection Calabi–Yau Spaces, *Nucl. Phys.* **B433** (1995) 501–554, hep-th/9406055.
- [19] P.S. Aspinwall, B.R. Greene and D.R. Morrison, Measuring Small Distances in $N=2$ Sigma Models, *Nucl. Phys.* **B420** (1994) 184–242, hep-th/9311042.
- [20] P.S. Aspinwall, Resolution of Orbifold Singularities in String Theory in *Mirror Symmetry II*, *AMS/IP Studies in Adv. Math.* **1**, B.R. Greene and S.-T. Yau (eds.), A.M.S., Providence/International Press, Cambridge (1997) 355–379, hep-th/9403123.
- [21] A. Klemm, P. Mayr and C. Vafa, BPS States of Exceptional Non-Critical Strings, in *Advanced Quantum Field Theory*, J. Fröhlich *et al.* (eds.), *Nucl. Phys.* **B** (Proc. Suppl.) **58** (1997) 177–194, hep-th/9607139.
- [22] W. Lerche, P. Mayr and N.P. Warner, Non-Critical Strings, del Pezzo Singularities and Seiberg–Witten Curves, *Nucl. Phys.* **B499** (1997) 125–148, hep-th/9612085.
- [23] A. Klemm and E. Zaslow, Local Mirror Symmetry at Higher Genus, hep-th/9906046.

- [24] K. Mohri, Y. Ohtake and S.-K. Yang, Duality Between String Junctions and D-Branes on Del Pezzo Surfaces, hep-th/0007243.
- [25] *Higher Transcendental Functions*, Vol. I, The Bateman Manuscript Project, A. Erdélyi (ed.), McGraw-Hill, New York (1953).
- [26] E.T. Whittaker and G.N. Watson, *A Course of Modern Analysis*, fourth edition, Cambridge Univ. Press, Cambridge (1927).
- [27] J.A. Minahan, D. Nemeschansky and N.P. Warner, Partition Functions for BPS States of the Non-Critical E_8 String, *Adv. Theor. Math. Phys.* **1** (1998) 167–183, hep-th/9707149.
- [28] See, for instance, *From Number Theory to Physics*, M. Waldschmidt *et al.* (eds.), Springer-Verlag, Berlin (1995); K. Kato, N. Kurokawa and T. Saito, *Number Theory 1*, *Translations of Mathematical Monographs* **186**, Amer. Math. Soc., Providence, (1999).
- [29] F. Rodriguez Villegas, Modular Mahler Measures I, in *Topics in Number Theory in Honor of B. Gordon and S. Chowla*, Mathematics and its Applications **467**, S.D. Ahlgren *et al.* (eds.), 17–48, Kluwer Academic Publishers, Dordrecht (1999); also visit <http://www.ma.utexas.edu/users/villegas>.
- [30] D.W. Boyd, Mahler’s Measure and Special Values of L -Functions, *Experiment. Math.* **7** (1998), 37–82 ; see also <ftp://math.ubc.ca/pub/boyd/mahler>.
- [31] P. Candelas, X.C. de la Ossa, P.S. Green and L. Parkes, A Pair of Manifolds as an Exactly Soluble Superconformal Theory, *Nucl. Phys.* **B359** (1991) 21–74.
- [32] H. Ooguri, Y. Oz and Z. Yin, D-Branes on Calabi–Yau Spaces and Their Mirrors, *Nucl. Phys.* **B477** (1996) 407–430, hep-th/9606112.
- [33] B.R. Greene and Y. Kanter, Small Volumes in Compactified String Theory, *Nucl. Phys.* **B497** (1997) 127–145, hep-th/9612181.

- [34] A. Klemm, W. Lerche and P. Mayr, K3-Fibrations and Heterotic-Type II String Duality, *Phys. Lett.* **B375** (1995) 313–322, hep-th/9506112.
- [35] B.H. Lian and S.-T. Yau, Arithmetic Properties of Mirror Map and Quantum Coupling, *Commun. Math. Phys.* **176** (1996) 163–191. hep-th/9411234.
- [36] J.H. Conway and S.P. Norton, Monstrous Moonshine, *Bull. London Math. Soc.* **11** (1979) 308–339.
- [37] M. Kohno, *Global Analysis in Linear Differential Equations*, Mathematics and its Applications **471**, Kluwer Academic Publishers, Dordrecht (1999).
- [38] B.H. Lian and S.-T. Yau, Mirror Maps, Modular Relations and Hypergeometric Series I, hep-th/9507151.
- [39] H. Kanno and S.-K. Yang, Donaldson–Witten Functions of Massless N=2 Supersymmetric QCD, *Nucl. Phys.* **B535** (1998) 512–530, hep-th/9806015.
- [40] C. Deninger, Deligne Periods of Mixed Motives, *K-Theory and the Entropy of Certain \mathbb{Z}^n -Actions*, *J. Amer. Math. Soc.* **10** (1997), 259–281.
- [41] Y.-K. E. Cheung and Z. Yin, Anomalies, Branes and Currents, *Nucl. Phys.* **B517** (1998) 69–91, hep-th/9710206.
- [42] R. Minasian and G. Moore, *K* Theory and Ramond-Ramond Charge, *JHEP* **9711** (1997) 002, hep-th/9710230.
- [43] T. Hauer and A. Iqbal, Del Pezzo Surfaces and Affine 7-Brane Backgrounds, *JHEP* **0001** (2000) 043, hep-th/9910054.
- [44] K. Hori, A. Iqbal and C. Vafa, D-Branes And Mirror Symmetry, hep-th/0005247.
- [45] R.P. Horja, Hypergeometric Functions and Mirror Symmetry in Toric Varieties, math.AG/9912109.
- [46] S. Hosono, Local Mirror Symmetry and Type IIA Monodromy of Calabi–Yau Manifolds, *Adv. Theor. Math. Phys.* **4** (2000), hep-th/0007071.

- [47] J.-M. Drezet and J. Le Potier, Fibrés Stables et Fibrés Exceptionnels sur \mathbb{P}_2 , Ann. Scient. Éc. Norm. Sup. **18** (1985) 193–244.
- [48] A.N. Rudakov, The Markov Numbers and Exceptional Bundles on \mathbf{P}^2 , Math. USSR Izv. **32** (1989) 99–112.